ECCC RECOMMENDATIONS - VOLUME 5 Part Id [Issue 1]

RECOMMENDATIONS FOR THE ASSESSMENT OF CREEP DUCTILITY DATA FOR USE IN DUCTILITY EXHAUSTION METHODS

blank page

ECCC RECOMMENDATIONS - VOLUME 5 Part Id [Issue 1]

RECOMMENDATIONS FOR THE ASSESSMENT OF CREEP DUCTILITY DATA FOR USE IN DUCTILITY EXHAUSTION METHODS

PREPARED BY A SUB-GROUP OF ECCC-WG1

Dr S R Holdsworth	EMPA, Switzerland (1992-2011, 2014-) [Past Convenor]	
Dr P F Morris	TATA Steel, UK (2000-7)	
Mr M W Spindler	EDF Energy, UK (2006-)	[Convenor, 2011-]

EDITED BY: M W SPINDLER

APPROVED D.J. Allen **DATE 07/05/2014**

On behalf of ECCC

blank page

ABSTRACT

ECCC Recommendations Volume 5 Part Id provides guidance for the assessment of large creep rupture ductility data sets. In common with the assessment procedures for creep rupture data assessment (CRDA) (Volume 5 Part 1a) this assessment procedure for creep ductility assessment (CDA) make use of post assessment tests for the physical realism of the model, and the goodness of fit within the range of the data. However, to date no consideration has been give to tests for stability and repeatability on extrapolation. Therefore the investigator is advised to ensure that the selected model remains physically realistic over the how applications range.

The guidance is based on the outcome of a four year work programme involving the evaluation of a number of assessment procedures by three analysts using 3 large working data sets on 2¼Cr1Mo, 11CrMoVNbN and Esshete 1250. However, for Issue 1 of Part Id only the work on one of these datasets 11CrMoVNbN has been prepared for the ECCC Recommendations and this work was intended for the specific application of producing creep ductility models for use in the ductility exhaustion approach for calculating creep damage. It is expected that future issues of Part 1d will provide further examples of the application of the procedures and further possible applications of ductility data. There is currently no requirement for long-time rupture ductility values in Design and Product Standards, but this is likely to change. Furthermore, long time rupture ductility values, or $A_u(T, \dot{\varepsilon}_f, \sigma, t)$ or $Z_u(T, \dot{\varepsilon}_f, \sigma, t)$ representations are already required for strain limit and ductility exhaustion calculations that are used for in-house design and life assessment procedures, in particular in the power generation industry.

ECCC Recommendations Volume 5 Part Id user feedback is encouraged and should be sent to:

Mr M W Spindler [ECCC-WG1 Convenor]
EDF Energy,
Barnett Way, Barnwood,
Gloucester GL4 3RS, UK.
Tel: +44 1452 653733
Fax: +44 1452 653025
E-mail: mike.spindler@edf-energy.com

ECCC may from time to time re-issue this document in response to new developments. The user is advised to consult the Document Controller for confirmation that reference is being made to the latest issue.

CONTENTS

RECOMMENDATIONS FOR THE ASSESSMENT OF CREEP DUCTILITY DATA FOR USE IN DUCTILITY EXHAUSTION METHODS

1. INTRODUCTION

The aim of the statistical analysis of creep ductility data, as described in this appendix, is to provide a description of the ductility as a function of the parameters that are used in ductility exhaustion approaches for the calculation of creep damage arising during displacement and strain controlled creep dwells. In particular, in the R5 ductility exhaustion approach [1] the ductility is treated as a function of strain rate and temperature. The creep damage is calculated from

$$d_c^{R5} = \int_0^{t_h} \frac{\dot{\varepsilon}_f}{\varepsilon_u(\dot{\varepsilon}_f, T)} dt \qquad \textbf{(1)}$$

where t_h is the dwell time, $\dot{\varepsilon}_f$ is the instantaneous creep strain rate and $\varepsilon_u(\dot{\varepsilon}_f, T)$ is the corresponding creep ductility at the appropriate temperature, T, as a function of the creep strain rate. Ideally, the relationship between creep ductility, the strain rate and the temperature, $\varepsilon_u(\dot{\varepsilon}_f, T)$, would be derived from constant strain rate tests over a wide range of strain rates and temperatures. Unfortunately, such data are rarely available and in R5 [1] it is usual for creep rupture data to be used, where the strain rate is defined by ε_u/t_u.

When the creep ductility is independent of the creep strain rate Eq. (1) simplifies to

$$d_c^{R5} = \frac{\varepsilon_f}{\varepsilon_u(T)} \qquad \textbf{(2)}$$

Recently it has been shown that improved predictions of creep damage can be obtained using the 'stress modified' ductility exhaustion approach [2,3,4,5] in which the creep damage is calculated from

$$d_c^{SM} = \int_0^{t_h} \frac{\dot{\varepsilon}_f}{\varepsilon_u(\dot{\varepsilon}_f, \sigma, T)} dt \qquad \textbf{(3)}$$

where $\varepsilon_u(\dot{\varepsilon}_f, \sigma, T)$ is the creep ductility at the appropriate temperature as a function of both the creep strain rate and the stress, σ, at the appropriate temperature. It is also conceivable that for some materials the creep ductility will be a function of stress and temperature (and independent of strain rate). For the 'stress modified' ductility exhaustion, the relationship between ductility, the strain rate, stress and the temperature, $\varepsilon_u(\dot{\varepsilon}_f, \sigma, T)$, can be derived using the engineering stress in creep rupture tests and by defining the strain rate by ε_u/t_u.

The above models for creep damage are used both for analysing the results of creep-fatigue tests and for performing plant life assessments. For the former it is necessary to have a model for the mean creep ductility and for the latter it is necessary to have a conservative model for creep ductility (for example a lower 95% confidence interval). Thus, the aims of a creep ductility assessment CDA are twofold:

- The first aim is to produce the most appropriate model for the mean creep ductility as a function of either; (i) the temperature, (ii) the creep strain rate and temperature, (iii) the stress and temperature or (iv) the creep strain rate, stress and temperature.
- The second aim is to define the lower 95% confidence interval, to the chosen model.

If a single CDA is performed on a material then this should be considered as an 'in-formal' assessment, for the purposes of producing an ECCC data sheet. When two independent CDAs

have been performed the preferred assessment can be considered as a 'formal' assessment, for the purposes of producing an ECCC data sheet.

2. THE DEFINITION OF CREEP DUCTILITY

In the current version of R5 [1] the definition of creep ductility that is used to calculate creep damage using the ductility exhaustion approach is the engineering creep strain at failure, which is given by the elongation at failure, A_u, minus the initial plastic loading strain, ε_i. This definition of creep ductility is used because in austenitic stainless steels A_u often contains both ε_i and creep strain, ε_f. This is particularly true for tests on austenitic steels at relatively low temperatures such as 550 and 600°C, which are often conducted above the proof stress. The engineering creep strain at failure is used in R5 because in cases were the creep ductility is treated as a function of the strain rate, then it would be non-conservative to include ε_i, which occurs at very high strain rates, with the creep strain at failure, which occurs at much lower strain rates. The engineering creep strain at failure (in absolute units) will hereafter be defined as ε_{fu} and is defined as $A_u/100 - \varepsilon_i$. Section 2.1 describes method that can be used to estimate ε_i from elevated temperature tensile tests.

Nevertheless, for cases where a lower bound creep ductility is used that is independent of the strain rate then it does not matter that A_u often contains a component of ε_i. This is not currently an option in R5.

In general it is found that ductility exhaustion approaches that use either ε_{fu} or A_u give conservative estimates of creep damage at failure in creep-fatigue tests. Holdsworth [6] has suggested that a less pessimistic value of creep damage can be calculated using the local strain at failure, which is calculated from the reduction in area, Z_u. This is not currently an option in R5. The true total local strain at failure, $\varepsilon_{tu(true)}$, can be calculated from

$$\varepsilon_{tu(true)} = \ln\left(\frac{1}{1 - Z_u/100}\right) \qquad \textbf{(4)}$$

and the corresponding true creep local strain at failure, $\varepsilon_{fu(true)}$, can be calculated from

$$\varepsilon_{fu(true)} = \ln\left(\frac{1}{1 - Z_u/100}\right) - \ln\left(1 + \varepsilon_i\right) \qquad \textbf{(5).}$$

Any of these four definitions of creep ductility may be used in an ECCC CDA. Whichever is chosen must be clearly stated, with its units (percent or absolute). For simplicity the chosen definition will be represented by the generalised symbol ε_u in much of this procedure.

In addition to the creep rupture data, it may be appropriate to collate the elevated temperature tensile data. In particular, values for proof stresses, R_{pX}, ultimate tensile strength, R_m, A and Z. Nevertheless, it is also necessary to know the strain rate, displacement rate or the loading rate of the tests.

2.1 Initial Plastic Loading Strain

For continuous strain measurement tests, in which the initial plastic loading strains have been measured this should always be used to calculate ε_{fu}. However, for simple stress rupture tests and interrupted strain measurement tests the initial plastic loading strains are not routinely measured. Nevertheless, ε_i can be estimated from 'heat specific' elevated temperature tensile properties. There are a number of approaches that can be used depending on what elevated temperature tensile properties are available. Which ever approach is used should be clearly described in the assessment report.

2.1.1 Heat Specific $R_{p0.1}$, R_{p1} and R_m

In this approach ε_i (in absolute units) is given by

$$\varepsilon_i = \left(\frac{\sigma_0 - R_{p0.1}}{K} \right)^{\frac{1}{\beta}} \quad \textbf{(6)}$$

where σ_0 is the test stress in MPa and $R_{p0.1}$ is the 0.1% proof stress at the test temperature. The constants K and β are calculated from tensile data on the same heat of material and at the same temperature at which the rupture test was conducted. From Eq. (6) and by interpolating between the 1% proof stress, $\sigma_{1\%}$, and the ultimate tensile strength, R_m, it can be shown that

$$\log(K) = \frac{\log(\varepsilon_m).\log(R_{p1} - R_{p0.1}) - \log(0.01).\log(R_m - R_{p0.1})}{\log(\varepsilon_m) - \log(0.01)} \quad \textbf{(7a)}$$

and that

$$\beta = \log\left(\frac{R_{p1} - R_{p0.1}}{K} \right) \Big/ \log(0.01) \quad \textbf{(7b)}$$

where ε_m is the strain at R_m in absolute units. This can be measured in the tensile test or if the value of ε_m is not available then an appropriate value can be determined by comparing observed and predicted values for ε_i, which have been measured during continuous strain measurement tests. It can be noted that a value of 0.265 (absolute units) has been found to give a good estimate of ε_i in Type 316H stainless steel.

2.1.2 Heat Specific $R_{p0.2}$, R_{p1} and R_m

If $R_{p0.1}$ is not known then the initial plastic loading strains can be estimated using:

$$\varepsilon_i = \left(\frac{\sigma_0}{K} \right)^{\frac{1}{\beta}} \quad \textbf{(8)}$$

where for test stresses below the 1% proof stress β and K are calculated from the heat specific 0.2% and 1% proof stresses using

$$\log(K) = \frac{\log(0.01).\log(R_{p0.2}) - \log(0.002).\log(R_{p1})}{\log(0.01) - \log(0.002)} \quad \textbf{(9a)}$$

and

$$\beta = \log\left(\frac{R_{p0.2}}{K} \right) \Big/ \log(0.002) \quad \textbf{(9b)}$$

For strains above 1% β and K are obtained from the 1% proof stresses and the ultimate tensile strength, using

$$\log(K) = \frac{\log(\varepsilon_m).\log(R_{p1}) - \log(0.01).\log(R_m)}{\log(\varepsilon_m) - \log(0.01)} \quad \textbf{(10a)}$$

and

$$\beta = \log\left(\frac{R_{p1}}{K} \right) \Big/ \log(0.01) \quad \textbf{(10b)}$$

The value of ε_m can be measured in the tensile test or if the value of ε_m is not available then an appropriate value can be determined by comparing observed and predicted values for ε_i, which have been measured during continuous strain measurement tests.

2.1.3 Heat Specific R_{pX} and R_m

For cases where only a single proof stress is known R_{pX}, which can be either $R_{p0.2}$ or R_{p1} the initial plastic loading strain can be calculated from Eq. (8):

where

$$\log(K) = \frac{\log(\varepsilon_m).\log(R_{pX}) - \log(0.002 \; or \; 0.01).\log(R_m)}{\log(\varepsilon_m) - \log(0.002 \; or \; 0.01)} \qquad \textbf{(11a)}$$

and

$$\beta = \log\left(\frac{R_{pX}}{K}\right) \Big/ \log(0.002 \; or \; 0.01) \qquad \textbf{(11b)}$$

The value of ε_m can be measured in the tensile test or if the value of ε_m is not available then an appropriate value can be determined by comparing observed and predicted values for ε_i, which have been measured during continuous strain measurement tests.

2.1.4 No Heat Specific Tensile Data

If heat specific tensile data are not available then the value of ε_i may be estimated using the mean material specific tensile properties from any of the three methods described above.

3. PRE-ASSESSMENT

It is anticipated that most ECCC CDAs will be performed on data sets that have been previously collated for a creep rupture data assessment CRDA. In addition to the requirements of a CRDA, plots of; (i) log ε_u versus σ_0 (or log σ_0), (ii) log ε_u versus T (or 1/T), (iii) log ε_u versus log t_u, (iv) log ε_u versus log ε_u/t_u and (v) log ε_u/t_u versus log σ_0, should be produced. In these plots different symbols and/or colours should be used to identify the secondary independent variables such as temperature, heat number or product form etc. These plots will be used to identify excessive scatter, outlying data points and outlying heats. The reasons for excluding any individual data points or heats should be fully documented. The plots will also be used to identify the candidate creep ductility models (Section 4.3) and to perform the post assessment tests or PATs (Section 5).

Since creep strain rate and stress will inevitably be highly inter-correlated it is helpful to analyse data from a range of temperatures. Ideally, the matrix of tests would have a range of stresses and temperatures, with the same stresses being used at all temperatures. Unfortunately this is not practicable as tests at high stresses and temperatures would fail due to tensile failure rather than creep and tests at low stresses and temperatures would last for unacceptably long durations. This means that temperature and stress will also show some degree of inter-correlation. The inter-correlation of the variables should be pre-assessed by producing a correlation matrix for all of the variables to be used in the CDA (i.e. log ε_u, log σ_0, 1/T, log t_u and log ε_u/t_u). High correlation coefficients (those closest to unity) between the independent variables log σ_0, 1/T, log t_u and log ε_u/t_u should be noted. There are no definitive rules that define what values should be considered as high. Nevertheless, the two highest values (ignoring the sign) should be noted and any other values that are above 0.7 (ignoring the sign). Any values that are below 0.5 (ignoring the sign) and high values between log t_u and log ε_u/t_u can be ignored.

4. ASSESSMENT OF CREEP DUCTILITY DATA

4.1 The Dependent Variable

The dependent variable (or response variable) in a CDA will often be the logarithm of the creep ductility, log ε_u. The units used for ε_u should be clearly stated. The base of the logarithm should be clearly stated (usually either $\log_{10}$ or $\log_e$ (ln), although for this procedure these will be generically referred to as log). It should be noted that when a least squares regression is used to determine the creep ductility model the use of log ε_u assumes a log-normal error distribution, which is often found to hold true for creep rupture data. Nevertheless, the assessor is advised to test this hypothesis at the end of the assessment (see Section 4.5).

4.2 The Independent Variables

The independent variables[1] that can be used for a CDA are appropriate functions of the variables that appear in the creep damage models[2]; log σ_0, 1/T and log ε_u/t_u and also log t_u. The units used for each of these variables should be clearly stated.

It is useful for the CDA to identify the principal independent variable. The principal independent variable is the most important of the independent variables or the only one. It is generally illuminating to treat log ε_u/t_u as the principal independent variable. Nevertheless, the principal independent variable can also be identified by:

- The application that the creep ductility model will be used for. For example if the outcome of the CDA has been pre-defined as a model for log ε_u as a function of 1/T alone then 1/T is the principal independent variable. Similarly, if the outcome of the CDA has been pre-defined as a model for log ε_u as a function of log ε_u/t_u and 1/T then log ε_u/t_u is the principal independent variable. If the outcome of the CDA has been pre-defined as a model for log ε_u as a function of log σ_0 and 1/T then log σ_0 is the principal independent variable. If the outcome of the model is predefined as a function of log ε_u/t_u, log σ_0 and 1/T then the appropriate principal independent variable would be log ε_u/t_u.
- If the CDA is unconstrained by a specific application then the principal independent variable can be defined by the variable that has the greatest influence on the model. In the first instance this can be determined visually from the plots of; (i) log ε_u versus σ_0 (or log σ_0), (ii) log ε_u versus T (or 1/T), (iii) log ε_u versus log t_u and (iv) log ε_u versus log ε_u/t_u. Alternatively, it could be determined as the independent variable that shows the highest correlation value with the dependent variable. However, if 1/T gives the highest correlation with log ε_u then the correlation between 1/T and log σ_0 should also be checked. If this is high then it is advisable to treat log σ_0 as the principal independent variable, rather than 1/T.

4.3 Identify Candidate Creep Ductility Models.

Changes to the creep failure mechanism often have a more pronounced effect on the creep ductility than they do on the rupture strength. These effects are often apparent when the creep ductility[3] is plotted versus the principal independent variable, although it may be necessary to use different symbols and or colours for the secondary independent variables such as temperature. By

---

[1] An independent variable, otherwise known as an explanatory variable or an x-variable, is one that influences the result of the test, in this case the creep ductility.

[2] Creep ductility models as a function of the rupture time (temperature and stress) can also be used to calculate creep damage, since these can be manipulated to give the creep ductility as a function of the average strain rate.

[3] It may also be useful to include the data from elevated temperature tensile tests; plotted as A or ln(1/(1-Z/100)) versus the test strain rate or R_m (to match the principal independent variable).

identifying the different failure regions it is possible to construct a list of suitable models for creep ductility. The different failure regions can be categorised by whether the creep ductility is; (i) independent of the principal independent variable, (ii) decreases as the principal independent variable decreases or (iii) increases as the principal independent variable decreases. There may also be more than one region of each type and these might be contiguous. For example the slope of the log ε_u versus log ε_u/t_u might change at a particular value. The appropriate creep ductility models for these types of behaviour are:

- For creep ductility (and tensile ductility) being independent of strain rate and/or stress but being a function of the temperature[4]:

$$\log \varepsilon_u = \alpha_0 + Q_0/T \quad \textbf{(12)}$$

- For creep ductility decreasing with decreasing strain rate or stress or decreasing with increasing rupture time[5]:

$$\log \varepsilon_u = \alpha_1 + m_1 \log(\sigma_0) + Q_1/T \quad \textbf{(13a)}$$

or $$\log \varepsilon_u = \alpha_1 + n_1 \log(\varepsilon_u / t_u) + Q_1/T \quad \textbf{(13b)}$$

or $$\log \varepsilon_u = \alpha_1 + l_1 \log(t_u) + Q_1/T \quad \textbf{(13c)}$$

or $$\log \varepsilon_u = \alpha_1 + n_1 \log(\varepsilon_u / t_u) + m_1 \log(\sigma_0) + Q_1/T \quad \textbf{(13d)}$$

or $$\log \varepsilon_u = \alpha_1 + l_1 \log(t_u) + m_1 \log(\sigma_0) + Q_1/T \quad \textbf{(13e)}$$

- It may also be appropriate to introduce combinations of two independent variables, when the slope changes with temperature, such as:

$$\log \varepsilon_u = \alpha_2 + m_2 \log(\sigma_0) + Q_2/T + S_2 \log(\sigma_0)/T \quad \textbf{(14a)}$$

or $$\log \varepsilon_u = \alpha_2 + n_2 \log(\varepsilon_u / t_u) + Q_2/T + S_2 \log(\varepsilon_u / t_u)/T \quad \textbf{(14b)}$$

or $$\log \varepsilon_u = \alpha_2 + l_2 \log(t_u) + Q_2/T + S_2 \log(t_u)/T \quad \textbf{(14c)}$$

- If the creep ductility increases with decreasing strain rate or stress or if creep ductility increases with increasing rupture time, then it is necessary to also consider the plot of log ε_u/t_u versus log σ_0. If log ε_u/t_u shows a sinh type of behaviour with log σ_0, i.e. log ε_u/t_u curves upwards at high stresses and towards the y-axis at low stresses, then it may not be necessary to use a different model to describe the creep ductility behaviour. If this is the case then Eq. (13d) should be used as it should be sufficient to describe both the decreasing log ε_u with decreasing log ε_u/t_u (at intermediate log ε_u/t_u) and increasing log ε_u with decreasing log ε_u/t_u (at low log ε_u/t_u). If log ε_u/t_u shows a power law type of behaviour with log σ_0, i.e. log ε_u/t_u versus log σ_0 lie on straight lines, then models that are functions of strain rate or rupture time may not be physically realistic. Thus, only functions of stress and temperature are advised, such as:

$$\log \varepsilon_u = \alpha_3 + m_3 \log(\sigma_0) + Q_3/T \quad \textbf{(15)}$$

or Eq. (14a)

For materials that show two or more different behaviours the creep ductility models should be combined using logical statements to produce a single model that describes the whole behaviour.

[4] Other functions of temperature may be used such as polynomials.

[5] Note; the average strain rate and the rupture time can not be used in the same model, as the rupture time cancels out.

- For instance, combining Eqs. (12) and (13x) or (14x) would describe a material for which the creep ductility (and tensile ductility) was independent of strain rate and/or stress at high values (an upper shelf) and then decreased with decreasing strain rate and/or stress at intermediate and low values. An appropriate combination would be:

$$\log \varepsilon_u = MIN\left[Eq.(12), \left(Eq.(13x)\ or\ Eq.(14x)\right)\right] \quad \textbf{(16)}$$

- In some materials a lower shelf creep ductility is reached. In this situation, the creep ductility (and tensile ductility) is independent of strain rate and/or stress at high values (an upper shelf) and then decreases with decreasing strain rate and/or stress at intermediate values and then is independent of strain rate and/or stress at low values. An appropriate combination would be:

$$\log \varepsilon_u = MAX \begin{Bmatrix} MIN\left[Eq.(12), \left(Eq.(13x)\ or\ Eq.(14x)\right)\right] \\ Eq.(12) \end{Bmatrix} \quad \textbf{(17)}$$

  where the first Eq. (12) describes the upper shelf and the second Eq. (12) describes the lower shelf. Thus, the coefficients will be different.

- In some materials a minimum creep ductility is reached. In this situation, the creep ductility (and tensile ductility) is independent of strain rate and/or stress at high values and then decreases with decreasing strain rate and/or stress at intermediate values and then increases with decreasing strain rate and/or stress at low values. If $\log \varepsilon_u/t_u$ shows a power law type of behaviour with $\log \sigma_0$, i.e. $\log \varepsilon_u/t_u$ versus $\log \sigma_0$ lie on straight lines, then an appropriate combination would be:

$$\log \varepsilon_u = MAX \begin{Bmatrix} MIN\left[Eq.(12), \left(Eq.(13x)\ or\ Eq.(14x)\right)\right] \\ MIN\left[Eq.(12), \left(Eq.(15)\ or\ Eq.(14a)\right)\right] \end{Bmatrix} \quad \textbf{(18)}$$

  where both of the occurrences of Eq. (12) describes the upper shelf and should have the same coefficients.

- When a minimum ductility occurs and $\log \varepsilon_u/t_u$ shows a sinh type of behaviour with $\log \sigma_0$, then it has been found that

$$\log \varepsilon_u = MIN\left[Eq.(12), Eq.(13d)\right] \quad \textbf{(19)}$$

  provides an adequate and physically realistic prediction of creep ductility.

- Equations (16) to (19) should be considered to be the preferred combinations of creep ductility models. Nevertheless, other combinations are admissible, so long as they are justified by the PATs and they perform better in the model criticism and selection procedures than Eqs. (16) to (19).

4.4 Model Fitting

The models that describe a single failure mechanism Eqs. (12), (13x), (14x) and (15) can be fitted to the data by using multiple linear regression. For materials that show two or more different failure mechanisms the combined creep ductility models (Eqs. (16) to (19)) can be fitted using non-linear regression techniques. One of the main difficulties with non-linear regression is in identifying realistic starting values for the constants. These starting values can be determined by using multiple linear regression to perform initial analysis for each of the mechanisms independently. This might involve splitting the data into sets that conform to a particular failure region, i.e. whether the creep ductility is; (i) independent of the principal independent variable, (ii) decreases as the principal independent variable decreases or (iii) increases as the principal independent variable decreases.

4.5 Model Criticism and Selection

It is expected that a number of different models will be identified as being suitable. Indeed, only by considering a number of different models can the assessor be confident that the best one has been selected. These models will subsequently be compared using model criticism and model selection procedures. These procedures consider which of the models provides the best fit to uniaxial creep ductility data. However, the procedures only consider which of the models provides the best fit to the data and can not prove that the model is physically correct. In addition, these procedures may reject physically correct models if either; (i) the independent variables are correlated (Section 3), (ii) there are insufficient data with the relevant test conditions or (iii) there are insufficient data that fail with a particular mechanism. Also it may be found that the model selection was highly influenced by a small number of data. If this is the case then the pre-assessment should be revisited to consider removing these data from the assessment.

The model criticism and model selection procedures follow statistical principles and also examine the visual realism of the models. The standard error of the prediction is used to show which of the models provides the best fit to the data. In addition, the Student's t-test is used to determine whether the values of the individual coefficients were significant at a 5% level. The visual realism of the models is checked by comparing the observed and predicted ductilities on a number of different graphs. The physical realism of the models can to a limited extent also be checked by the same graphs. However, it is also advisable to check that the values of the coefficients are close to the theoretical values, that are defined later in this section.

The standard error of the prediction is given by:

$$S.E. = \sqrt{\frac{\sum_i \left(\log \varepsilon_{u\,i} - \log \varepsilon_{u\,i}^{*}\right)^2}{\text{residual degrees of freedom}}}$$

where the residual degree of freedom is the total number of data points minus the number of coefficients in the creep ductility model. In general, the model with the lowest S.E. will give the best fit to the data. However, some of the coefficients may not be significant.

To test whether individual coefficients are significant it is advised to use the Student's t-test at a 5% level. Most analysis packages provide the 'P-value', which is the probability that the coefficient is zero. P-values that are less than 0.05 are thus significant at the 5% level and those that are greater than 0.05 are not significant at the 5% level. Coefficients that are not significant should be removed from the model and the model should be re-fitted to the data. For example, if the P-value for S_1 in Eqs. (14x) is greater than 0.05 then the model should revert to one of the Eqs. (13x), type of models. In addition, it is often found that the coefficient α_1 in Eqs. (13d) and (13e) is not significant and can be set to zero.

The model fitting methods described in Section 4.4 are based on least squares methods and assume that the random errors are log-normally distributed, i.e. log ε_u is the dependent variable. If the scatter is not log-normally distributed then this can indicate that either; (i) the creep ductility model is incorrect or (ii) that the error distribution is incorrect. Many analysis packages include tests for normality, which can be used. Otherwise a histogram of the residuals (log ε_u-log ε_u*) can be visually inspected. If the data are not log-normally distributed then the assessor might consider either; (i) repeating the CDA with a different model for which the log-normal error distribution is applicable, (ii) using ε_u as the dependent variable or (iii) using other analysis techniques, for example maximum likelihood methods, in which different error distributions can be used (i.e. log-logistic or Weibull)[6].

[6] The shape of the histogram of residuals can be used as a guide to a more appropriate error distribution.

The visual realism of the models can be checked by plotting graphs of; (i) log ε_u versus the principal independent variable, which show the data and the predictions, (ii) the observed creep ductility, log ε_u, versus predicted creep ductility, log ε_u*, which show different subsets of data (eg. temperature) and (iii) residual (log ε_u-log ε_u*) versus the secondary independent variables and other variables not used in the model, e.g. 1/T, log t_u etc.

- For the graphs of log ε_u versus the principal independent variable, it is necessary to use symbols and/or colour to separate the data at different temperatures. Alternatively, if log ε_u/t_u (or log t_u), log σ_0 and 1/T have been treated as independent variables then it is necessary to produce plots for each of the principal test temperatures and to use symbols and/or colour to separate the data and predictions at different stresses (or a range of stresses). These plots also form the basis of PAT D1.1 (Section 5).
- Graphs of observed log ε_u, versus predicted log ε_u*, graphs should show subsets of data (eg. temperature) and should include fits to the data at individual test temperatures. These plots also form the basis of PAT D2.2 (Section 5).
- Graphs of residual (log ε_u-log ε_u*) versus the secondary independent variables can be particularly useful in identifying important variables that have not been included in the model. It is advisable to use symbols and/or colour to separate the data at different temperatures. For example, residual versus log t_u will identify if the model needs to include the effects of rupture time. In addition, residual versus heat number will identify outlying heats that do not behave like the rest of the data.

The physical realism of the models can, to a limited extent, also be checked by the same graphs. However, it is also advisable to check that the values of the coefficients are close to the theoretical values. These values are based on theoretical models for creep ductility that are described in [2,3,7,8]. It should be noted that these theoretical values are not necessarily the same in each equation (13x) or (14x). For guidance:

- The value of m_1 (in Eq. (13a)) might be typically less than or approximately equal to n/2-1[7] and should be neither negative nor greater than n-1.
- The value of n_1 (in Eqs. (13b) and (13d)) might be typically less than or approximately equal to (n-1)/n but should be neither negative nor greater than 1.
- The values of m_1 (in Eq. (13d)) and m_3 (in Eq. (15)) might be typically -n/2 but should be neither positive nor less than -n.
- The values of l_1 (in Eqs. (13c) and (13e)) might be typically greater than or approximately equal to 1-n and should be neither positive nor less than 1-2n.
- The values of m_1 (in Eq (13e)) might be typically greater than or approximately equal to $-n^2/2$ and should be neither positive nor less than $-n^2$.
- In Eq. (14a) the value of (m_2+S_2/T) might be typically -n/2 but should be neither positive nor less than –n.
- In Eq. (14b) the value of (n_2+S_2/T) might be typically less than or approximately equal to (n-1)/n but should be neither negative nor greater than 1.
- In Eq. (14c) the value of (l_2+S_2/T) might be typically greater than or approximately equal to 1-n and should be neither positive nor less than 1-2n.

[7] Where n is the stress exponent for power law minimum creep rate and is typically 3 to12 for engineering steels.

Values of n_1, m_1 or m_3 that are not physically realistic might be the result of high correlation between two or more variables (see correlation matrix). If this is the case the analysis can be repeated after assuming the theoretical values for either;

- l_1 1-n in Eqs. (13c) and (13e),
- m_1 n/2-1 in Eq. (13a),
- m_1 -n/2 in Eq. (13d),
- m_1 $-n^2/2$ in Eq (13e),
- n_1 (n-1)/n in Eqs. (13b) and (13d) or
- m_3 -n/2 in Eq. (15).

However, models that include assumed theoretical values should not be used unless they (i) pass the PATs and (ii) can be validated by applying them to calculate creep damage in creep-fatigue tests.

5. POST ASSESSMENT TESTS

The model criticism and selection procedures are related to post assessment tests, PATs, although in that part of the assessment they are used for guidance only. Formal PATs for CDA assessment fall into two categories:

- The visual/physical realism of the predicted creep ductility.
- The effectiveness of the model prediction within the range of the data.

PAT-D1.1 The physical realism of the models should be checked visually by plotting $\log \varepsilon_u$ versus the principal independent variable; it is necessary to use symbols and/or colour to separate the data at different temperatures. Alternatively, if $\log \varepsilon_u/t_u$ (or $\log t_u$), $\log \sigma_0$ and 1/T have been treated as independent variables then it is necessary to produce plots for each of the principal test temperatures and to use symbols and/or colour to separate the data and predictions at different stresses (or a range of stresses).

The predicted model should give a credible fit to the data at all conditions.

PAT-D2.1 The goodness of fit within the range of the data should be assessed using plots of observed $\log \varepsilon_u$ versus predicted $\log \varepsilon_u$*. This PAT includes fitting a straight line through all the observed versus predicted creep ductility data. Which is used to assess the fit within the range of the data. A second use for PAT D2.1 is to assess the scatter of the chosen model. This is done using 95% confidence intervals[8]. The data should be reassessed if either:

The slope of the fitted line is less than 0.9 or greater than 1.1 or if the intercept is less than –0.3 or greater than 0.3.

There are more than 5% of the data outside either of the 95% confidence intervals.

PAT-D2.2 The goodness of fit at individual temperatures is assessed using a graph of the observed $\log \varepsilon_u$ versus predicted $\log \varepsilon_u$*, which shows data at individual temperatures and which includes fits to the data at individual test temperatures. This graph also includes the 95% confidence intervals and the data should be reassessed if:

[8] The 95% confidence intervals are given by $\log \varepsilon_u = \log \varepsilon_u^* \pm$ S.E.x(the inverse of Student's t-distribution for the relevant residual degrees of freedom and a two sided probability of 0.05).

The fitted lines to the individual temperatures do not lie within the 95% confidence intervals, over the range of the predicted values for the whole data set.

6. RECOMMENDATIONS FOR CHOOSING A PREFERRED ASSESMENT

When two independent CDAs have been performed, using either the above procedure or an alternative, the preferred assessment can be considered as a 'formal' assessment, for the purposes of producing an ECCC data sheet. Procedures that can be used to choose between assessments are only qualitative and semi-quantitative. Both models should pass the CDA PATs (see Section 5). If both CDAs used least squares regression (log-normal error distribution) and there were no assumptions regarding the theoretical values of the coefficients, then the model with the lowest S.E. should be considered as the 'shortlisted' model. If (i) a method other than least squares regression were used, (ii) the error distribution is not log-normal or (iii) the fit included theoretical values for the coefficients, then specialist judgement may be exercised to select the preferred model. Also the same specialist judgements should be used before the 'shortlisted' model becomes the preferred model. These specialist judgements should also be used to ensure that:

- The model does not predict unrealistically high or low values of creep ductility, for conditions outside the range of the data. This can be checked by extending the predictions on the graphs for PAT D1.1 beyond the range of the data. Models that contain both upper and lower shelves or an upper shelf and a minimum will be preferred. This is because unrealistic values are not possible.
- Preference should be given the CDAs that have been validated by applying it them to calculate creep damage in creep-fatigue tests on the same material. If this is not the case then models that are based on a type of equation that has a proven track record on other materials, should be preferred.

7 REFERENCES

1 R5, Assessment Procedure for the High Temperature Response of Structures Issue 3, British Energy, Gloucester, UK, June 2003.

2 M W Spindler, An Improved Method for Calculation of Creep Damage During Creep–Fatigue Cycling, Materials Science and Technology Vol. 23 No. 12, pp. 1461-1470, 2007.

3 M W Spindler, The prediction of creep damage in Type 347 weld metal: Part I. The determination of material properties from creep and tensile tests. Int. J. Pressure Vessels & Piping., Vol. 82, No. 3, pp. 175–184, 2005.

4 M W Spindler, The Prediction of Creep Damage in Type 347 Weld Metal: Part II Creep Fatigue Tests, Int. J. Pressure Vessels & Piping., Vol. 82, No. 3, pp. 185-194, 2005.

5 M W Spindler, Effects of Dwell Location on The Creep-Fatigue Endurance of Cast Type 304L, Mater. High Temp., Vol. 25, No. 3, pp. 91-100, 2008.

6 S R Holdsworth, Prediction of Creep-Fatigue Behaviour at Stress Concentrations in 1CrMoV Rotor Steel, in Life Assessment and Life Extension of Engineering Plant, Structures and Components, EMAS, UK, 1996.

7 M W Spindler, R Hales and R P Skelton, The Multiaxial Creep Ductility of an Ex-Service Type 316H Stainless Steel, Proc. of the 9th Int. Conf. on Creep & Fracture of Engineering Materials & Structures, ed. J D Parker, IOM London, UK, 2001.

8 M W Spindler, The Multiaxial and Uniaxial Creep Ductility of Type 304 Steel as a Function of Stress and Strain Rate, Mater. at High Temps. Vol. 21, pp. 47–52, 2004.

APPENDIX A

CREEP DUCTILITY OF 11CRMOVNBN BOLTING STEEL
A1 - Development of Guidance for The Assessment of Creep Rupture Ductility Data for ECCC

M W Spindler [EDF Energy]

blank page

Appendix A - APPENDIX A DEVELOPMENT OF GUIDANCE FOR THE ASSESSMENT OF CREEP RUPTURE DUCTILITY DATA FOR ECCC

M W Spindler

1 INTRODUCTION

The high alloy steel 11CrMoVNbN (for which the current specification is X19CrMoNiNbVN11-1 [1]) is used for bolting in steam turbines with operating temperatures of up to 580°C. 11CrMoVNbN has a higher relaxation strength than the alternative 12CrMoV bolting steel X22CrMoV12-1 [1]. However, the creep ductility of 11CrMoVNbN is lower than that of X22CrMoV12-1 and 11CrMoVNbN sufferers from notch weakening, when creep tested with a circumferencial 'V' notch. Nevertheless, 11CrMoVNbN has been successfully used for 35-45 years as a material for high temperature fasteners and has been found to be immune from creep cracking in the first engaged thread. This is largely due to the use of material that conforms to the X19CrMoNiNbVN11-1 specification, which has limited Al contents and has been austenitised in the range 1100 to 1130°C [2].

As part of the activities of the European Creep Collaborative Committee, ECCC, Working Group 1 the creep ductility data for 11CrMoVNbN have been statistically analysed using a variety of different models for creep ductility. The purpose of these analyses have been to develop preferred methods for analysing creep ductility data and to make recommendations to ECCC regarding the preferred procedures for the analysis, the post assessment (see Appendix A1) and the presentation of creep ductility data (see Appendix B).

The aim of the statistical analysis of creep ductility data, as applied by EDF Energy, is to provide a description of the ductility as a function of the parameters that are used in ductility exhaustion approaches for the calculation of creep damage arising during strain controlled creep dwells. In particular, in the R5 ductility exhaustion approach [3] the ductility is treated as a function of strain rate and temperature. The creep damage is calculated from

$$d_c^{R5} = \int_0^{t_h} \frac{\dot{\varepsilon}_c}{\varepsilon_f(\dot{\varepsilon}_c, T)} dt \qquad \textbf{(1)}$$

where[1] t_h is the dwell time, $\dot{\varepsilon}_c$ is the instantaneous creep strain rate and $\varepsilon_f(\dot{\varepsilon}_c, T)$ is the corresponding creep strain at failure at the appropriate temperature, T, as a function of the creep strain rate.

Recently it has been shown that improved predictions of creep damage can be obtained using the 'stress modified' ductility exhaustion approach [4,5] in which the creep damage is calculated from

$$d_c^{SM} = \int_0^{t_h} \frac{\dot{\varepsilon}_c}{\varepsilon_f(\dot{\varepsilon}_c, \sigma, T)} dt \qquad \textbf{(2)}$$

where $\varepsilon_f(\dot{\varepsilon}_c, \sigma, T)$ is the creep strain at failure at the appropriate temperature as a function of both the creep strain rate and the stress. Like the R5 ductility exhaustion approach the 'stress modified' ductility exhaustion approach requires the model for the creep ductility to include a function of the strain rate.

Ideally, the relationship between ductility, the strain rate and the temperature, $\varepsilon_f(\dot{\varepsilon}_c, T)$, would be derived from constant strain rate tests over a wide range of strain rates and temperatures. Unfortunately, such data are rarely available and in R5 [3] it is suggested that creep rupture data can

[1] Please note the nomenclature used in this Appendix does not comply with ECCC Volume 2. Nevertheless, all terms are defined in this Appendix.

be used, where the strain rate is defined by ε_f/t_r, where t_r is the rupture time. For the 'stress modified' ductility exhaustion approach constant strain rate data are not amenable to simplified analysis to derive the relationship between ductility, the strain rate, stress and the temperature, $\varepsilon_f(\dot{\varepsilon}_c, \sigma, T)$. This is because the stress varies during a constant strain rate test. Hence, it is usual to use the engineering stress in creep rupture tests and to define the strain rate by ε_f/t_r.

It has been shown that for strain controlled creep dwells the ductility exhaustion approach in conjunction with relationships for $\varepsilon_f(\dot{\varepsilon}_c, T)$ consistently gives reasonable predictions of creep damage at failure. Furthermore, improved predictions of creep damage can be achieved when the 'stress modified' ductility exhaustion approach is used in conjunction with relationships for $\varepsilon_f(\dot{\varepsilon}_c, \sigma, T)$. However, the use of the average strain rate, ε_f/t_r, to analyse the data presents a problem for the statistical analysis of rupture ductility data. This is because ε_f is treated both as the dependent variable and as a component of one of the independent variables. This leads to misleadingly good fits to the data and to relatively low standard errors. In this report some alternative statistical analysis strategies are investigated that are intended to avoid the problems of using the average strain rate when analysing rupture ductility data.

- The time to failure will be used rather than the average creep strain rate. However, even this approach suffers from the problem that time to failure is a result of a creep test and is not truly an independent variable. Furthermore, the time to failure is subject to considerable random variation (typically one or two orders of magnitude). Regression analyses strictly assume that the independent variables are not subject to random variation. This means that the results of regression analyses that use the time to failure as an independent variable may not give the optimum fit to the data.
- The variation of the time to failure and the average creep strain rate will be modelled in terms of 'metallurgical variables' such as chemical composition, heat treatment and room temperature tensile properties. These 'metallurgical variables' are truly independent between different heats of material and can thus the treated as independent variables. The creep rupture ductility will then be fitted as a function of the predicted time to failure or the predicted average creep strain rate, rather than using the observed values.

It should be noted that as an alternative to using the measured creep ductility as a function of the average creep strain rate it is proposed in [4] that the instantaneous strain rate during the creep test can be used. This method uses a reverse modelling approach to determine the coefficients in a creep damage model, which calculates creep damages distributed about unity for creep and tensile test data. The approach uses the instantaneous true inelastic strain rate and the true stress as calculated from the available creep curves and stress strain data from tensile tests and thus avoids the problems associated with using the average strain rate. However, the reverse modelling approach requires detailed deformation data, which are not commonly available and are not available for 11CrMoVNbN steel. Thus, this method will not be considered further in this report.

2 DATA FOR 11CrMoVNbN STEELS

The data that were used for this investigation were provided by ECCC Working Group 1 as one of the group's working data sets. The chemical composition, heat treatment and room temperature tensile properties of the 11CrMoVNbN materials are given in Table 1. It should be noted that none of the heats meet the requirements for the current specification for X19CrMoNiNbVN11-1 [1]. In particular, the solution/normalisation temperatures of the tested materials are too high and the carbon contents are too low. Nevertheless, the heats fall within the general classification of 11CrMoVNbN steels.

The stress rupture data for 11CrMoVNbN contained 217 data on 18 heats and the extent of the data is summarised in Table 2. It should be noted that heats 14, 24, 32 and 33 conform to the Jethete M160 specification, which is different from the other specifications in that it contains greater Ni contents.

The ductility data for 11CrMoVNbN from tensile tests were obtained from [6]. These tensile ductility data were used to improve the fits to the upper shelf ductility. The data for tensile ductility contained 37 data, 10 at 400°C, 9 at 500°C, 3 at 550°C, 9 at 600°C and 6 at 700°C.

3 ANALYSIS OF RUPTURE DUCTILITY DATA

The data on 11CrMoVNbN have been analysed using both multiple linear regression and non-linear regression techniques. Multiple linear regression was used to determine the effects of the average strain rate, $\dot{\varepsilon}_{AV}$, the temperature, T, the stress, σ, and the rupture time, t_r, on the creep ductility, ε_f. The average strain rate is defined here as ε_f/t_r. Non-linear regression was used to include an upper shelf into the model for ductility as a function of $\dot{\varepsilon}_{AV}$, T and σ. It should be noted that a lower shelf ductility has not been used in any of the models reported here. It is clear from Figures 1, 2 and 4 that the ductility data for 11CrMoVNbN show a large amount of scatter and that there are no clear trends of ductility with $\dot{\varepsilon}_{AV}$, T or t_r. However, Figure 3 shows that there is a trend of increasing ductility with decreasing stress.

3.1 Multiple Linear Regression

The effects of $\dot{\varepsilon}_{AV}$, T, σ and t_r on ductility have been determined after taking natural logarithms of the appropriate variables. Thus, the dependent variable was $\ln(\varepsilon_f)$ in absolute values and the independent variables were $\ln(\dot{\varepsilon}_{AV})$ in 1/h, 1/T in Kelvin, $\ln(\sigma)$ in MPa and $\ln(t_r)$ in hours. Different combinations of these independent variables can be combined to give the following expressions for rupture ductility

$$\ln(\varepsilon_f) = \ln(A_1) + \frac{\Delta G_{AC}}{RT} + n_1 \ln(\dot{\varepsilon}_{AV}) + m_1 \ln(\sigma) \tag{3}$$

and

$$\ln(\varepsilon_f) = \ln(A_1) + \frac{\Delta G_{AC}}{RT} + m_1 \ln(\sigma) + l_1 \ln(t_r) \tag{4}$$

The values for the coefficients $\ln(A_1)$, $\Delta G_{AC}/R$, n_1, m_1 and l_1 were then determined using multiple linear regression. The independent variables $\ln(\dot{\varepsilon}_{AV})$ and $\ln(t_r)$ can not be combined in the same equation as the $\ln(t_r)$ term in each cancels out. Different combinations of independent variables were fitted to the data so that the most appropriate factors that affect ductility could be determined. The results of the data analysis are summarised in Table 3. It should be noted that when an independent variable has not been considered the constant is shown as zero. Also included in the table is the standard error of the model, which is used to judge how well the models fit the data.

It is clear from the values of standard error that a model in which the ductility is function of $\ln(\dot{\varepsilon}_{AV})$, 1/T and $\ln(\sigma)$ (Eq. (3), Model 5) gives the best prediction of the data (i.e. it shows the lowest standard error, see Table 3). This is shown graphically in Figure 5.

3.2 Non-Linear Regression

It was noted from Figure 5 that Model 5, which is based on a function of $\ln(\dot{\varepsilon}_{AV})$, 1/T and $\ln(\sigma)$ overestimates many of the ductility values when these values are large. This is because the simple application of multiple linear regression can not take account of the effect of changes to the failure mechanism on the creep ductility. In the case of the 11CrMoVNbN data a change occurs at high strain rates where the ductility shows an upper shelf value which is independent of strain rate and stress. This can be seen in the high strain rate data shown in Figure 1. Changes in failure mechanism can be modelled by using non-linear regression techniques. It should be noted that a transgranular (shear or cup and cone) fracture would be expected on the upper shelf and intergranular fracture would be expected when the ductility was a function of $\ln(\dot{\varepsilon}_{AV})$ and $\ln(\sigma)$.

The creep ductility data for 11CrMoVNbN have been fitted by using non-linear regression with logical statements to return the upper shelf value when the prediction of Eq. (3) is greater than the value of the upper shelf and otherwise the logical statement returns the value from Eq. (3). This can be written as

$$\ln(\varepsilon_f) = \text{MIN}\left[\ln(A_1) + \frac{\Delta G_{AC}}{RT} + n_1 \ln(\dot{\varepsilon}_{AV}) + m_1 \ln(\sigma), \quad \ln(\varepsilon_U) \right] \tag{5}$$

where the natural logarithm of the upper shelf ductility, $\ln(\varepsilon_U)$, is treated as an independent variable. The values for the coefficients $\ln(A_1)$, $\Delta G_{AC}/R$, n_1, m_1 and the upper shelf ductility, ε_U, are summarised in Table 3.

It can be seen from the standard errors for the non-linear regression analyses that the inclusion of an upper shelf (Model 6) improves the fit to the data (i.e. this reduces the standard error). This is shown graphically in Figure 5. However, there are relatively few data on the upper shelf and as a consequence it has been assumed here that the ductility on the upper shelf is independent of temperature. This assumption gives problems when predicting the elongation at 450°C. This can be seen in Figure 6, which shows that Eq. (5), Model 6, gives a good prediction of the elongation at 475 to 600°C but is poor at predicting the behaviour at 450°C. The problem with the elongation at failure at 450°C is caused by an effect of temperature on the upper shelf ductility and is because the 450°C data are actually independent of strain rate (see Figure 1) and should have been modelled as being on the upper shelf. This can be achieved by the use of a model that allows the upper shelf ductility to predict low ductilities at low temperatures and higher ductilities at higher temperatures. The problem for any analysis is that creep rupture data rarely contain sufficient data that fail on the upper shelf to define such a relationship. Nevertheless, the results of tensile tests could be a suitable source of upper shelf ductility data. It can be seen from Figure 7 that tensile data in 11CrMoVNbN do indeed show an appropriate effect of temperature on ductility. In addition, it can be seen from Figure 8 that the tensile ductility data at 400°C are consistent with the creep ductility data at 450°C, i.e. the tensile data and the creep ductility data that are on the upper shelf show similar ductilities.

The inclusion of a temperature effect on the upper shelf ductility can be simply achieved by including an activation energy term into the upper shelf ductility. The creep rupture ductility data and the tensile ductility data have been combined and the following equation fitted to the combined data set

$$\ln(\varepsilon_f) = \text{MIN}\left[\ln(A_1) + \frac{\Delta G_{AC}}{RT} + n_1 \ln(\dot{\varepsilon}_{AV}) + m_1 \ln(\sigma), \quad \ln(B) + \frac{C}{T} \right] \tag{6}$$

It can be seen from Figure 9 and Table 3 that the inclusion of a temperature effect on the upper shelf ductility gives a better fit to the data than the previous models.

3.3 True Local Strain at Failure

Initially the elongation at failure was used as the measure of ductility. However, work conducted for the Brite C-FAT project showed that a "Local" strain at failure, which was calculated from the Reduction of Area, gave better predictions of creep-fatigue damage at failure than the elongation at failure [7]. Thus, in this report three models that showed low standard errors when applied to the elongation at failure data (Eqs. (3) and (5)) have also been applied to the True Local strain at failure, ε_{Ltrue}, which is given by

$$\varepsilon_{Ltrue} = \ln\left(\frac{1}{1 - RofA} \right) \tag{7}$$

where the reduction of area and the local strains are in absolute units.

The results of these analyses are shown in Table 3 and Figure 10, Figure 11 and Figure 12. It should be noted that the improvements to the fit that were obtained are similar to those described for the elongation at failure.

4 ANALYSIS USING METALLURGICAL VARIABLES

As an alternative to using the observed values of average strain rate or the observed time to failure it is proposed here that predicted values for the average strain rate can be used. The predicted values are not subject to random variation and consequently can be used as independent variables. To give an effective prediction of creep ductility the predicted values of average strain rate will need to describe

the random variation in creep strength. Otherwise, the creep ductility predictions would be very much worse than the predictions made using the observed values of average strain rate. A significant proportion of the random variation in creep strength arises from heat to heat variations. It is therefore necessary to produce models that describe the effects of 'metallurgical variables' on the average strain rate.

The 'metallurgical variables' that are available include the chemical composition of the specified elements, the heat treatment temperatures and the room temperature tensile properties (see Table 1). However, Al and B were not treated as 'metallurgical variables' since values were not available for many of the heats. For P, S, N, $R_{p0.2}$ and R_m a small number of heats had no values. In these cases the blank was replaced by the average value for all heats. This is judged to have no affect on the final models. Nevertheless, it does allow all of the heats to be included in the analyses. The effects of the 'metallurgical variables' have been determined using a backward elimination, stepwise regression procedure. The backward elimination method starts with the largest regression, using all variables and then reduces the number of variables until a decision is reached on the optimum equation. Variables have been excluded that fail the Student's t-test at the 5% level. In addition, metallurgical judgement and knowledge of the correlation of some of the 'metallurgical variables' have been used to add physical realism to the backward elimination method.

The correlation matrix for the 'metallurgical variables' is shown in Table 4, from which it may be seen that there are strong correlations between $R_{p0.2}$ and R_m, which is not surprising and also between Mn and V. Hence, models that include both $R_{p0.2}$ and R_m have been avoided and since V is expected to strongly influence creep strength, whereas Mn is not, Mn has been excluded from many analyses. The analyses using the metallurgical variables involved fitting only the rupture data. This was because elevated temperature tensile data were not available for all of the heats. Thus, the upper shelf has been treated as being independent of temperature.

4.1 Average Strain Rate

The first stage of the approach has been to model the average strain rate as a function of the stress and temperature and the metallurgical variables. This is intended to describe the random variation in creep strength. An examination of the data for average strain rate versus stress (see Figure 13) shows that an exponential law is more appropriate than a power law, since the data do not lie on straight lines when plotted on log axes. An exponential law approximates to a sinh law for a wide range of stresses and although a sinh law would be more correct the exponential law is assumed as it simplifies the analysis procedures. Further examination of the behaviour of individual heats, shows that at low stresses the average strain rate becomes independent of stress (see Figure 14). This is a transitory effect caused by the ductility increasing by the same factor as the time to failure (see Figure 15). This has been modelled with a modified form of the exponential law that is given by

$$\dot{\varepsilon}_{AV} = \varepsilon_f / t_r = A(\text{Materials Variables})\exp\left(\frac{\Delta G_A}{R.T}\right)\exp(n\sigma) + B(\text{Materials Variables})\exp\left(\frac{\Delta G_B}{R.T}\right) \qquad (8)$$

where ΔG_A, n and ΔG_B are the constants and A and B are functions of the materials variables (composition, heat treatment and tensile properties). To ensure that the intercepts in each of the functions of A and B were of modest magnitudes, A and B were defined as

$$A = \exp\left(\begin{matrix} a_0 + a_C.C + a_{Si}.Si + a_{Mn}.Mn + a_P.P + a_S.S + a_N.N + a_{Cr}.Cr + a_{Mo}.Mo \\ + a_{Nb}.Nb + a_{Ni}.Ni + a_V.V + a_{Soln}.Soln + a_{Age}.Age + a_{R0\_2}.R0\_2 + a_{Rm}.Rm \end{matrix}\right) \qquad (9a)$$

$$B = \exp\left(\begin{matrix} b_0 + b_C.C + b_{Si}.Si + b_{Mn}.Mn + b_P.P + b_S.S + b_N.N + b_{Cr}.Cr + b_{Mo}.Mo \\ + b_{Nb}.Nb + b_{Ni}.Ni + b_V.V + b_{Soln}.Soln + b_{Age}.Age + b_{R0\_2}.R0\_2 + b_{Rm}.Rm \end{matrix}\right) \qquad (9b)$$

where $a_{0,C..etc.}$ and $b_{0,C..etc.}$ are the constants and C, Si, etc. are the composition, heat treatment and tensile properties in weight %, °C and MPa respectively. The regression was carried out using $\ln(\dot{\varepsilon}_{AV})$ as the dependent variable, i.e. taking natural logarithms of equation (8). Due to a limitation in the statistical analysis software (only 25 independent variables could be considered in a single model), the combination of materials variables that describe A were determined initially and the materials variables that describe B were determined afterwards. Thus, the backward elimination

method started with $b_{0,C..etc.}$ set to zero. The materials variables $a_{0,C..etc.}$ that failed the t-test at the 5% level were excluded from the model by setting the coefficient to zero. The selected model is given by Eq. (10)

$$\dot{\varepsilon}_{AV} = A.\exp\left(\frac{-68029}{.T}\right)\exp(0.048837\sigma) + B.\exp\left(\frac{-8636.92}{.T}\right) \quad (10a)$$

$$A = \exp\left(\begin{matrix}32.155 - 15.553.C + 13.769.Si + 205.417.P + 189.76.N + 1.5838.Cr - 15.553.Mo \\ + 2.9551.Ni - 0.089122.Soln + 0.14677.Age\end{matrix}\right) \quad (10b)$$

$$B = \exp\left(\begin{matrix}131.77 - 3.4299.Si - 101.97.P - 0.85808.Cr + 7.88978.Mo \\ + 7.6303.Nb + 3.7524.Ni - 0.12189.Soln + 0.011380.R0\_2\end{matrix}\right) \quad (10c)$$

The observed strain rates are compared with the predicted strain rates in Figure 16, which also shows the predicted values for a simple exponential law. It can be seen from Figure 16 that Eq. (10) provides a significantly better fit to the data than the simple exponential law.

4.2 Time to Failure

It is also possible to use the materials variables to describe the scatter in rupture strength. For example the rupture strength of 11CrMoVNbN (Figure 17) can be described a third order Orr-Sherby-Dorn equation which is given by

$$\ln(t_r) = \beta_0 + \beta_1 \ln(\sigma) + \beta_2[\ln(\sigma)]^2 + \beta_3[\ln(\sigma)]^3 + \frac{\beta_4}{T} \quad (11)$$

where β_i are the constants. It is possible to include heat to heat variations in rupture strength into Eq. (11) by making β_0 a function of the materials variables.

$$\begin{aligned}\beta_0 = {} & c_0 + c_C.C + c_{Si}.Si + c_{Mn}.Mn + c_P.P + c_S.S + c_N.N + c_{Cr}.Cr + c_{Mo}.Mo \\ & + c_{Nb}.Nb + c_{Ni}.Ni + c_V.V + c_{Soln}.Soln + c_{Age}.Age + c_{R0\_2}.R0\_2 + c_{Rm}.Rm\end{aligned} \quad (12)$$

where $c_{0,C..etc.}$ are the constants and C, Si, etc. are the composition, heat treatment and tensile properties in weight %, °C and MPa respectively. As with the modelling of the average strain rate a backward elimination method was used. Variables have been excluded that fail the t-test at the 5% level. In addition, metallurgical judgement and knowledge of the correlation of some of the 'metallurgical variables' have been used to add physical realism to the backward elimination method. In particular Mn was taken out of the model rather than V, although the probability that c_V was zero for one of the trial models was larger than the probability that c_{Mn} was zero. The selected model is given by

$$\ln(t_f) = \beta_0 - 122.614\ln(\sigma) + 24.641[\ln(\sigma)]^2 - 1.6839[\ln(\sigma)]^3 + \frac{35776}{T} \quad (13a)$$

$$\beta_0 = 118.43 + 84.758.P + 0.85140.Cr - 4.6013.Ni - 9.0529.V + 0.038098.Soln + 9.0529\text{x}10^{-3}.R0\_2 \quad (13b)$$

The observed times to failure are compared with the predicted times to failure in Figure 17 and Figure 18, which also shows the predicted values for the Orr-Sherby-Dorn equation. It can be seen from Figure 18 that Eq. (13) provides a significantly better fit to the data than the Orr-Sherby-Dorn equation.

4.3 Strain at Failure

Previously, in Section 3 the observed average strain rate or the observed time to failure were used when fitting to Eqs. (3), (4) and (5). However, the average strain rate that is predicted from Eq. (10) can now be used instead of the observed average strain rate in Eqs. (3) and (5). This avoids the problem that the observed average strain rate is a function of the dependent variable. In the current work Eq. (3) was not used and only Eq. (5) was fitted using the predicted average strain rate.

In addition, the time to failure that is predicted from Eq. (13) has been used instead of the observed time to failure. This avoids the problem at the observed time to failure is subject to considerable

random variation and should not be treated as an independent variable in a regression analysis. To do this Eq. (4) has been modified in the same way that Eq. (3) was modified by the inclusion of the upper shelf ductility to give

$$\ln(\varepsilon_f) = \text{MIN}\left[\ln(A_1) + \frac{\Delta G_{AC}}{RT} + l_1 \ln(t_f) + m_1 \ln(\sigma), \quad \ln(\varepsilon_U) \right] \tag{14}$$

The coefficients that were derived for the fits to Eqs. (5) and (14) are given in Table 3. Plots of the observed versus the predicted creep ductility are given in Figure 19 and Figure 20.

The approach outlined above suggests that the analysis for creep ductility could be done in a single step. This can be carried out by substituting Eqs. (8) and (9) into Eq. (5) or by substituting Eqs. (11) and (12) into Eq. (14). Both of these would produce new equations that describe the creep ductility as a function of the independent variables, stress temperature and the metallurgical variables. However, such equations would include multiple temperature and stress terms, which would be co-linear. This means that it would not be possible for a regression analysis to separate the relative contributions of these terms and would give meaningless results. Nevertheless, this does not preclude the use of related models that could describe the creep ductility equations as a function of the independent variables, stress temperature and the metallurgical variables. This would also avoid any problems about the use of the average strain rate or the time to failure as independent variables.

As a demonstration of this in this report the data have been fitted to

$$\ln(\varepsilon_f) = \text{MIN}\left[\begin{array}{c} \ln(\varepsilon_U), \\ \left(\begin{array}{l} a_0 + a_C.C + a_{Si}.Si + a_{Mn}.Mn + a_P.P + a_S.S + a_N.N + a_{Cr}.Cr + a_{Mo}.Mo \\ + a_{Nb}.Nb + a_{Ni}.Ni + a_V.V + a_{Soln}.Soln + a_{Age}.Age + a_{R0\_2}.R0\_2 + a_{Rm}.Rm \\ + \beta_1 \ln(\sigma) + \beta_2 \left[\ln(\sigma)\right]^2 + \frac{\beta_3}{T} + \frac{\beta_4}{T^2} \end{array} \right) \end{array} \right] \tag{15}$$

As before a backward elimination method was used in which variables were excluded that failed the t-test at the 5% level. In addition, metallurgical judgement and knowledge of the correlation of some of the 'metallurgical variables' have been used to add physical realism to the backward elimination method. The selected model is given by

$$\ln(\varepsilon_f) = \text{MIN}\left[\begin{array}{c} -1.3656, \\ \left(\begin{array}{l} 74.742 - 37.005.C + 64.491.N + 0.38845.Cr \\ - 3.1349.Nb + 8.7173.V - 0.10202.Soln + 0.037825.Age \\ - 21.113 \ln(\sigma) + 1.7422 \left[\ln(\sigma)\right]^2 + \frac{113123}{T} - \frac{42581189}{T^2} \end{array} \right) \end{array} \right] \tag{16}$$

The results of this regression are also shown in Table 3 and the observed creep ductilities are compared with the predicted creep ductilities in Figure 21.

5 HEAT TO HEAT VARIATIONS IN CREEP DUCTILITY

When the observed average strain rate and the observed time to failure are used to fit the creep ductility data the effect of heat to heat variations on creep and rupture strength are implicitly taken into account by the model. Thus, the high creep strength heats give low ductilities and the low creep strength heats give high ductilities. This is shown by n_1 in equations (3), (5) and (6) being positive and l_1 in equations (4) and (14) being negative (see Table 3). This can be shown graphically in Figure 22, which plots the observed and predicted creep ductility versus the observed time to failure for Eq. (5) fitted using the observed average strain rate (Model 6). Figure 22 shows how Eq. (5) is able to implicitly take account of the heat to heat variations in creep ductility.

Analyses that use the 'metallurgical variables' explicitly take the effect of the heat to heat variations in creep strength, on the creep ductility, into account. This can be shown graphically in Figure 23, which plots the creep ductility versus the time to failure for Eq. (5) fitted using the predicted average strain rate (Model 11). It should be noted that in Figure 23 the predicted creep ductility has been

plotted versus a predicted time to failure, in which the time to failure is predicted from the predicted creep ductility divided by the predicted average strain rate from Eq. (10). Similarly, Figure 24 shows the creep ductility versus the time to failure for Eq. (14), which has been fitted using the predicted time to failure (Model 12). It should be noted that in Figure 24 the predicted creep ductility has been plotted versus a predicted time to failure, which is given by Eq. (13). Figure 25 shows the creep ductility for Eq. (16) versus the observed time to failure (Model 13).

It can be seen from Figures 22, 23, 24 and 25 that all of the models reflect the heat to heat differences in creep ductility. However, it is also clear that Eq. (14), which has been fitted using the predicted time to failure given by Eq. (13) (Model 12), is not as good as the other models. This is reflected in the standard errors of the creep ductility predictions that are shown in Table 3.

6 DISCUSSION

This report contains a number of analyses of the creep ductility data for 11CrMoVNbN. Many of the models are functions of the strain rate, stress and temperature (Eqs. (3), (5) and (6)). These models are used to calculate creep damage using the 'stress modified' ductility exhaustion approach, Eq. (2). The models that are functions of the time to failure, stress and temperature (Eqs. (4) and (14)) can also be used to calculate creep damage using the 'stress modified' ductility exhaustion approach. This is because Eq. (3) can be manipulated to give

$$\ln(\varepsilon_f) = \frac{\ln(A_1)}{(1-n_1)} + \frac{\Delta G_{AC}}{RT(1-n_1)} - \frac{n_1}{(1-n_1)}\ln(t_r) + \frac{m_1}{(1-n_1)}\ln(\sigma) \qquad (17)$$

Thus, the coefficients determined for Eqs. (4) and (14) can be manipulated to give coefficients for Eqs. (3), (5) and (6). Analyses that use $\ln(t_r)$ as an independent variable and not $\ln(\dot{\varepsilon}_{AV})$ avoid the problems that are caused by ε_f being treated as both the dependent variable and as a component of one of the independent variables.

However, the time to failure is a result of a creep test and is not an independent variable. Furthermore, the time to failure is subject to considerable random variation (typically one or two orders of magnitude). Regression analyses strictly assume that the independent variables are not subject to random variation. This means that the results of regression analyses that use the time to failure as an independent variable will not give the optimum fit to the data.

To overcome these problems the predicted values for the average strain rate or time to failure have been used. The predicted values are not subject to random variation and consequently can be used as independent variables. To give an effective prediction of creep ductility the predicted values of average strain rate need to describe the heat to heat variation in creep strength. Thus, models that describe the effects of 'metallurgical variables' on the average strain rate and time to failure have been determined using backward elimination, stepwise regression.

Alternatively, it would be necessary to use other advanced methods of multivariate analysis, such as:

- "Model II" regression, which allows both the dependent and independent variables to be subject to random variation.
- Partial Least Squares regression, which enables the relationship between a set of multivariate independent variables, such as stress, temperature and the 'metallurgical variables', and multivariate dependent variables, such as ductility and rupture time to be determined.

These options have not been attempted in this report, as the computing methods were not available to the author.

6.1 Effect of Stress and Strain Rate on Creep Ductility

The models described by Eqs. (3), (5) and (6) are not suitable to show on a two dimensional plot. Nevertheless, by restricting the plot to the main test temperature, 550°C, and colour coding tests with stresses in particular ranges to is possible to show how stress and strain rate affect the creep ductility of 11CrMoVNbN (see Figure 26). It can be seen from Figure 26 that for a given average creep strain rate the tests at low stresses show high ductilities and the tests at high stresses show low ductilities.

Considering that the creep strain rate is a function of the stress this variation can only be accounted for by heat to heat variations in creep strength behaviour. Such that the high strength heats fail with low ductilities and the low strength heats fail with high ductilities.

6.2 Analyses using Metallurgical Variables

In order to take account of the effect of heat to heat variations on the creep ductility, the variation of the time to failure and the average creep strain rate have been modelled in terms of the 'metallurgical variables'. This also enables the creep rupture ductility to be re-fitted as a function of the predicted time to failure or the predicted average creep strain rate, rather than using the observed values. Since the predicted time to failure and the predicted average creep strain rate are not subject to random error and are functions of only 'truly' independent variables, the problems of using the observed values are avoided. However, there are problems with each of these analyses that mean that none of them should be used for engineering assessments. These problems relate to a poor distribution of data used for the analyses. In particular, there are no data for either the Al content or for the residual elements, which are known to affect creep strength and creep ductility [2,8]. Nevertheless, it is suggested that the statistical techniques that have been used in this report or more advanced techniques, could be used to analyse data sets that have better distributions of data.

6.2.1 Average Strain Rate

The chosen model for the average creep strain rate, as function of stress temperature and the 'metallurgical variables' Eq. (10), gives a very much better fit to the data than a simple exponential law (see Figure 16). This shows that Eq. (10) takes account of a significant amount of the heat to heat variation in creep strength. Furthermore, many of the 'metallurgical variables' that were selected correspond with those that would be expected from metallurgical considerations. For example; C, Mo and solution treatment temperature decrease the creep rate, whereas Ni and aging temperature increase the creep rate. However, Eq. (10) includes the contributions from 17 'metallurgical variables' and yet there are data for only 18 heats. This means that the contributions from some of the 'metallurgical variables' might not be realistic. In these cases the regression procedure may be using differences between heats that do not affect creep strength, i.e. P, to describe large heat to heat variations in creep strength. The above considerations mean that Eq. (10) should not be considered as representing the true effect of 'metallurgical variables' on the average creep strain rate of 11CrMoVNbN steel. Nevertheless, the methods described in Section 4.1 could be applied successfully to data sets on materials where all of the significant 'metallurgical variables' are known and for which there are data on a large number of different heats of steel.

6.2.2 Time to Failure

Equation (13) provides a significantly better fit to the data than the Orr-Sherby-Dorn equation (see Figure 18). However, it is clear that the data plotted as observed time to failure versus predicted time to failure are better described by a curve than by a straight line. This suggests that there is a systematic error in the prediction given by Eq. (13). It is likely that the backward elimination method did not identify the optimum model to describe the rupture strength of 11CrMoVNbN. This is also suggested by the 'metallurgical variables' that were selected may not be realistic; for example Eq. (13) suggests that increasing V contents decreases the rupture strength. A more physically realistic model might possible if specific heats were excluded from the analysis. For example, heat 31 exhibits particularly low times to failure at high stresses, which might be the result of this heat being over tempered at 700°C (see Table 1). Furthermore, heats 22, 27, 29 and 34 conform to the Jethete M160 specification and contain significantly more Ni than the other 11CrMoVNbN heats. However, any reduction in the size of the data base will make it even more difficult to analyse using the 'metallurgical variables'. Nevertheless, it is probable that more advanced methods for multivariate analysis, such as partial least squares regression, would result in a more realistic model than the multiple linear regression technique that was used here.

An alternative method of using the analyses to predict the rupture strength of 11CrMoVNbN is to divide the predicted creep ductility by the predicted average strain rate (i.e. Eq. (5) divided by Eq. (10)). Indeed, this gives a better fit to the data than both the Orr-Sherby-Dorn equation and Eq. (13), see Figure 27, within the range of the data. Furthermore, a straight line describes the data plotted as

observed time to failure versus predicted time to failure. However, this approach can not be relied on for extended time extrapolation and should not be used to derive design strengths. Indeed, at low stresses the method predicts that the time to failure does not increase even though the stress decreases see Figure 28. This is caused by the conditions of stress and temperature for which; (i) the average strain rate is given by the last term in Eq. (10a), which is independent of stress (the first term in Eq. (10a) being negligible) and (ii) the creep ductility being on the upper shelf. Therefore, both the average strain rate and the creep ductility are independent of stress and consequently so are the predicted times to failure. Clearly, this is not physically realistic. This could be overcome by a further modification to the model for the average strain rate

$$\dot{\varepsilon}_{AV} = \varepsilon_f / t_r = A(\text{Materials Variables})\exp\left(\frac{\Delta G_A}{R.T}\right)\exp\left(n\left[\sigma - C(\text{Materials Variables}) + \frac{D}{T}\right]\right) + B(\text{Materials Variables})\exp\left(\frac{\Delta G_B}{R.T}\right) \quad (18)$$

However, initial trials with this approach showed that the model was very sensitive to small changes in the coefficients and could not be fitted to all heats at once. Nevertheless, the approach was successful when applied to a limited data set containing only two heats, see Figure 29.

6.2.3 Strain at Failure

The use of the predicted average strain rate or the predicted time to failure enables predictions of creep ductility to be made when only the independent variables; stress, temperature and the 'metallurgical variables' are known, as in Eq. (16). Equation (16) does indeed give a good fit the creep ductility data (see Figure 21). In addition, Eq. (16) describes many of the aspects of the heat to heat variations in creep ductility, see Figure 25, although it does not exhibit the increasing ductility shown a short times by heats 14, 25, 29 and 30. However, Eq. (16) would not be amenable to the calculation of creep damage, since the strain rate is not one of the variables.

6.3 Application to the Calculation of Creep Damage

The fits using the observed or the predicted strain rates and times to failure give rise to slightly different coefficients for Eqs. (3), (4), (5) and (6) (see Table 3). Since these models are used to calculate creep damage during creep-fatigue cycles, in order to show which of the models derived in this report gives the best prediction of creep damage, it would be necessary to analyse the results of creep-fatigue tests. This is outside the scope of this report. Nevertheless, it is clear from Figure 19 that the use of the predicted average strain rate gives a good fit the creep ductility data and describes many of the aspects of the heat to heat variations in creep ductility, see Figure 23.

7 CONCLUSIONS

1. This report contains a number of analyses of the creep ductility data for 11CrMoVNbN steel. Many of the models are functions of the strain rate, stress and temperature. These models are used to calculate creep damage using the 'stress modified' ductility exhaustion approach.

2. However, the use of the average strain rate to analyse the data presents a problem for the statistical analysis of rupture ductility data. This is because the creep ductility is treated both as the dependent variable and as a component of one of the independent variables. It has been shown that the time to failure can also be used rather than the average creep strain rate. Models that are functions of the time to failure, stress and temperature can also be manipulated so that they can be used to calculate creep damage. However, it would be necessary to validate this approach by analysing the results of creep-fatigue tests. This has not been attempted in this report.

3. It has been show that for a given average creep strain rate the tests at low stresses show high ductilities and the tests at high stresses show low ductilities. Considering that the creep strain rate is a function of the stress this variation can be accounted for by heat to heat variations in creep strength behaviour. Such that the high strength heats fail with low ductilities and the low strength heats fail with high ductilities.

4. Analysis approaches have been described that take account of the effect of heat to heat variations on the creep ductility, in terms of the 'metallurgical variables'. This also enables the creep rupture ductility to be re-fitted as a function of the predicted time to failure or the predicted average creep strain rate, rather than using the observed values. However, there are problems with each of these analyses that mean that none of them should be used for engineering assessments. These problems relate to a poor distribution of data used for the analyses. Nevertheless, it is suggested that the statistical techniques that have been used in this report or more advanced techniques, could be used to analyse data sets that have better distributions of data.

5. It has been shown that models for the creep ductility and the average strain rate, which take account of heat to heat variations by the use of 'metallurgical variables', can be used to predict the rupture strength. However, the specific models in this report can not be relied on for extended time extrapolation and should not be used to derive design strengths.

8 REFERENCES

1 EN 10269:2013, Steels and Nickel Alloys for Fasteners with Specified Elevated and/or Low Temperature Properties, 2013.

2 K H Mayer and H König, Operational Characteristics of 10-12% CrMoV Bolt Steels for Steam Turbines, in Performance of Bolting Materials in High Temperature Plant Applications, ed. A Strang, pp. 150-162, IOM, London, UK, 1995.

3 R5, Assessment Procedure for the High Temperature Response of Structures Issue 3, EDF Energy, Gloucester, UK, 2003.

4 M W Spindler, The prediction of creep damage in Type 347 weld metal: part 1. The determination of material properties from creep and tensile tests. Int. J. of Press. Vess. and Piping, Vol. 82, pp. 175–184, 2005.

5 M W Spindler, The Calculation of Creep Damage as a Function of Stress and Strain Rate, Int. Conf. on High Temperature Plant Integrity and Life Extension, Robinson College, Cambridge University, UK, 14 – 16 April 2004.

6 S M Plummer and P R McCarthy, Project 2021:Creep of Steels, 12% Cr Type Steels: High Temperature Properties, ERA Technology Report 2A/891 Revision 2, 1987.

7 S R Holdsworth, Prediction of Creep-Fatigue Behaviour at Stress Concentrations in 1CrMoV Rotor Steel, in Life Assessment and Life Extension of Engineering Plant, Structures and Components, EMAS, UK, 1996.

8 V Foldyna and Z Kubon, Consideration of the Role of Nb, Al and Trace Elements in Creep Resistance and Embrittlement Susceptibility of 9-12% Cr Steel, in Performance of Bolting Materials in High Temperature Plant Applications, ed. A Strang, pp. 173-187, IOM, London, UK, 1995.

9 TABLES

Table 1 Chemical Composition, Heat Treatment and Room Temperature Tensile Properties of 11CrMoVNbN Steels

Specification.	Note or Heat No.	Chemical Composition in wt %													Solution /Normalisation Temperature (°C)	Ageing/ Tempering Temp. (°C)	RT Tensile Props. (MPa)	
		C	Si	Mn	P	S	N	Cr	Mo	Nb	Ni	V	Al	B			$R_{p0.2}$	R_m
DIN 17240, 1976, X19CrMoNiNbVN11-1	min	0.12	0.20	0.40	-	-	0.030	10.00	0.50	0.20	0.30	0.18	-	-	1100	650	740	895
	max	0.20	0.70	1.00	0.035	0.015	0.080	11.50	0.90	0.55	0.80	0.35	-	-	1170	720	-	1050
EN 10269: 2013, X19CrMoNiNbVN11-1	min	0.17	-	0.40	-	-	0.05	10.00	0.50	0.25	0.20	0.10	-	-	1100	670	750	900
	max	0.23	0.5	0.90	0.025	0.015	0.10	11.50	0.80	0.55	0.60	0.30	0.020	0.0015	1130	720	-	1050
Firth Vickers 448E	Nominal	0.14	0.50	1.0	-	-	0.05	11.0	0.50	0.40	0.70	0.33		0.005	1160	675-700	-	-
Jethete M160	min	0.10	-	0.75	-	-	0.030	11.0	0.50	0.10	0.75	0.20	-	-	-	-	-	-
	max	0.20	0.35	1.20	0.030	0.030	0.090	13.0	0.70	0.40	1.25	0.40	-	-	-	-	-	-
Jessop Saville H46	Nominal	0.15	0.3	0.6	-	-	0.06	11.5	0.6	0.3	0.5	0.3	-	-	1150	680	-	-

Table 2 Distribution of Creep Rupture and Elevated Temperature Tensile Data for 11CrMoVNbN Steels

Temp (°C)	No. of Heats	No. of Tensile Data	Test Durations (hours)							
			<10,000	10,000 to 20,000	20,000 to 30,000	30,000 to 50,000	50,000 to 70,000	70,000 to 100,000	>100,000	t_{max}
400	9	10	-	-	-	-	-	-	-	-
450	3	-	2	2	1	-	-	-	-	20821
475	6	-	8	5	3	3	3	1	-	83929
500	9	9	23	5	5	3	3	3	1	128149
550	18	3	55	21	10	12	7	4	1	100538
600	6	9	19	7	2	4	3	1	-	94021
700	6	6	-	-	-	-	-	-	-	-
Total	18	37	107	40	21	22	16	9	2	4185493

Table 3 Results of Statistical Analyses of Creep Ductility data for 11CrMoVNbN Steels

Models Fitted Using the Observed Values of Average Strain Rate or the Observed Time to Failure														
Model	Ductility	Equation	Regression	Data	$\ln(A_1)$	n_1	$\Delta G/R$	m_1	l_1	Upper Shelf %	ln(B)	C	Degrees of freedom	Standard Error
1	Elong	(4)	Linear	Creep Only	-3.4886	0	472.91	0	0.0827	-	-	-	214	0.8225
2	Elong	(3)	Linear	Creep Only	-1.6339	0.1304	731.10	0	0	-	-	-	214	0.8009
3	Elong	(3)	Linear	Creep Only	-4.7123	0	7562.13	-1.2096	0	-	-	-	214	0.7261
4	Elong	(4)	Linear	Creep Only	-4.4800	0	12791.22	-2.0592	-0.2160	-	-	-	213	0.6826
5	Elong	(3)	Linear	Creep Only	-2.7926	0.3317	13083.81	-2.1130	0	-	-	-	213	0.5061
6	Elong	(5)	Non-Linear	Creep Only	-2.2514	0.4743	18976.09	-3.1913	0	25.66	-	-	212	0.4468
7	Elong	(6)	Non-Linear	Creep and Tensile	-2.6205	0.4817	19114.83	-3.1378	0	-	1.1085	-2166.7	248	0.4311
8	True Local	(3)	Linear	Creep Only	-2.1664	0.2961	3167.15	0	0	-	-	-	202	1.0249
9	True Local	(3)	Linear	Creep Only	-3.1905	0.4811	16878.39	-2.4950	0	-	-	-	201	0.6865
10	True Local	(5)	Non-Linear	Creep Only	-4.5179	0.7191	23306.40	-3.2009	0	94.10	-	-	200	0.5921
Models Fitted Using the Predicted Values of Average Strain Rate or the Predicted Time to Failure														
Model	Ductility	Equation	Regression	Data	$\ln(A_1)$	n_1	$\Delta G/R$	m_1	l_1	Upper Shelf %	Predicted $\ln(\dot{\varepsilon}_{AV})$ or $\ln(t_r)$ given by:		Degrees of freedom	Standard Error
11	Elong	(5)	Non-Linear	Creep Only	-1.5654	0.4285	17883.34	-3.1623	0	24.67	Eq. (10)		212	0.5390
12	Elong	(14)	Non-Linear	Creep Only	-3.3457	0	14436.31	-2.5650	-0.2459	25.93	Eq. (13)		212	0.7037
13	Elong	(16)	Non-Linear	Creep Only	See Equation (16)								204	0.4887

Table 4 Correlation Matrix for Elongation at Failure data for 11CrMoVNbN Steels (high correlations are shown in red bold).

	$\ln(\varepsilon_f)$	$\ln(t_f)$	$\ln(\dot{\varepsilon}_{AV})$	$\ln(\sigma)$	1/T	C	Si	Mn	P	S	N	Cr	Mo	Nb	Ni	V	Soln	Age	$R_{p0.2}$	R_m
$\ln(\varepsilon_f)$	1.00																			
$\ln(t_f)$	0.18	1.00																		
$\ln(\dot{\varepsilon}_{AV})$	0.28	**-0.89**	1.00																	
$\ln(\sigma)$	-0.31	-0.48	0.33	1.00																
1/T	0.04	0.06	-0.03	**0.72**	1.00															
C	-0.17	0.03	-0.11	-0.10	-0.10	1.00														
Si	0.00	-0.03	0.03	0.03	0.03	0.26	1.00													
Mn	0.07	0.00	0.03	-0.26	-0.19	0.11	0.16	1.00												
P	0.20	0.06	0.03	-0.05	-0.02	0.09	-0.51	-0.02	1.00											
S	0.04	0.03	-0.01	0.10	0.11	-0.12	-0.44	-0.38	0.46	1.00										
N	0.03	0.11	-0.09	-0.23	-0.19	0.42	-0.23	0.19	0.29	-0.10	1.00									
Cr	0.08	0.08	-0.04	-0.09	-0.04	-0.12	-0.41	0.28	0.27	0.16	0.30	1.00								
Mo	0.25	0.07	0.05	-0.03	0.02	0.15	0.03	-0.16	0.48	0.30	0.45	0.30	1.00							
Nb	-0.19	0.03	-0.11	0.01	-0.04	-0.05	0.43	0.29	-0.44	-0.34	-0.45	-0.50	-0.60	1.00						
Ni	0.12	-0.06	0.12	-0.08	0.02	-0.18	-0.52	0.36	0.37	0.32	0.24	0.65	0.16	-0.42	1.00					
V	0.23	0.01	0.09	-0.18	-0.12	0.06	0.28	**0.78**	0.20	-0.50	0.04	0.09	-0.01	0.31	0.10	1.00				
Soln	-0.38	-0.01	-0.17	-0.09	-0.07	-0.05	-0.22	0.38	-0.25	-0.06	0.06	0.37	-0.25	0.10	0.49	-0.09	1.00			
Age	0.09	-0.20	0.23	0.11	0.10	-0.40	0.17	-0.15	-0.32	-0.14	-0.60	-0.37	-0.15	0.14	-0.16	-0.09	0.06	1.00		
$R_{p0.2}$	-0.03	0.06	-0.07	-0.10	-0.06	0.06	-0.18	0.53	0.02	0.19	0.25	0.49	-0.09	0.08	0.61	0.20	0.44	-0.52	1.00	
R_m	-0.04	0.08	-0.10	-0.11	-0.04	0.23	-0.21	0.46	0.17	0.15	0.43	0.57	0.05	-0.05	0.68	0.20	0.39	-0.68	**0.90**	1.00

10 FIGURES

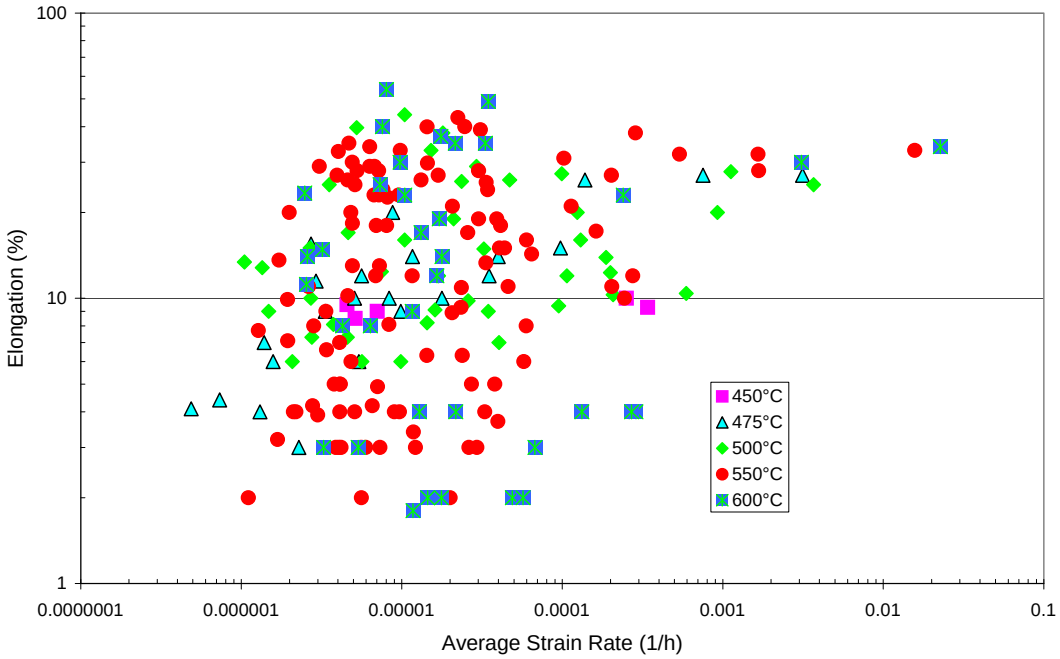

Figure 1 Elongation at Failure of 11CrMoVNbN as a Function of Average Strain Rate .

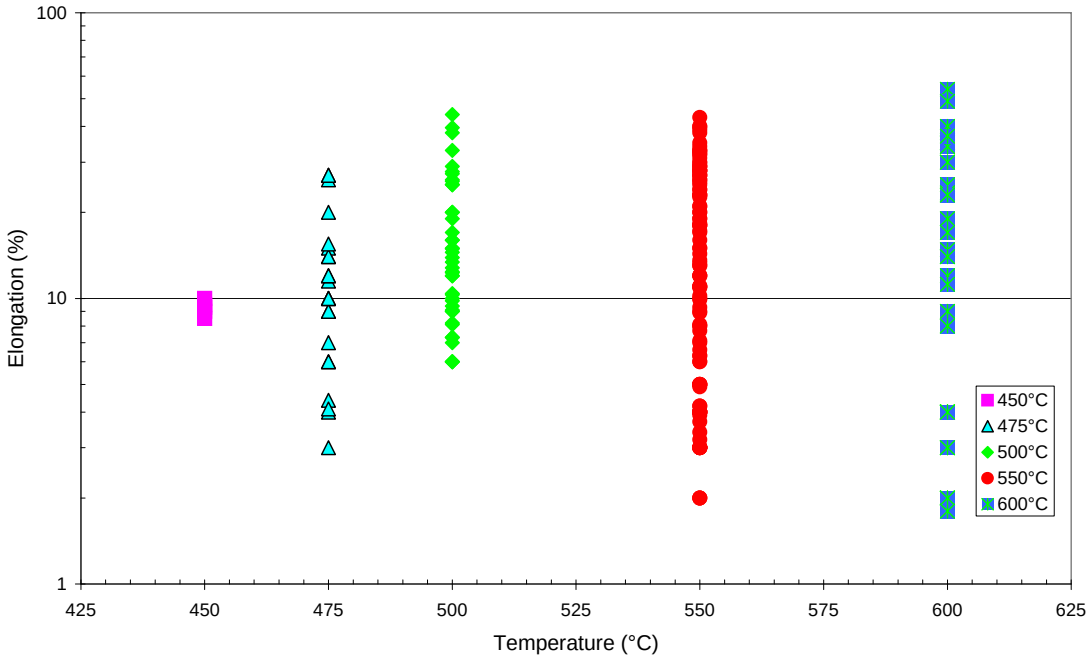

Figure 2 Elongation at Failure of 11CrMoVNbN as a Function of Temperature.

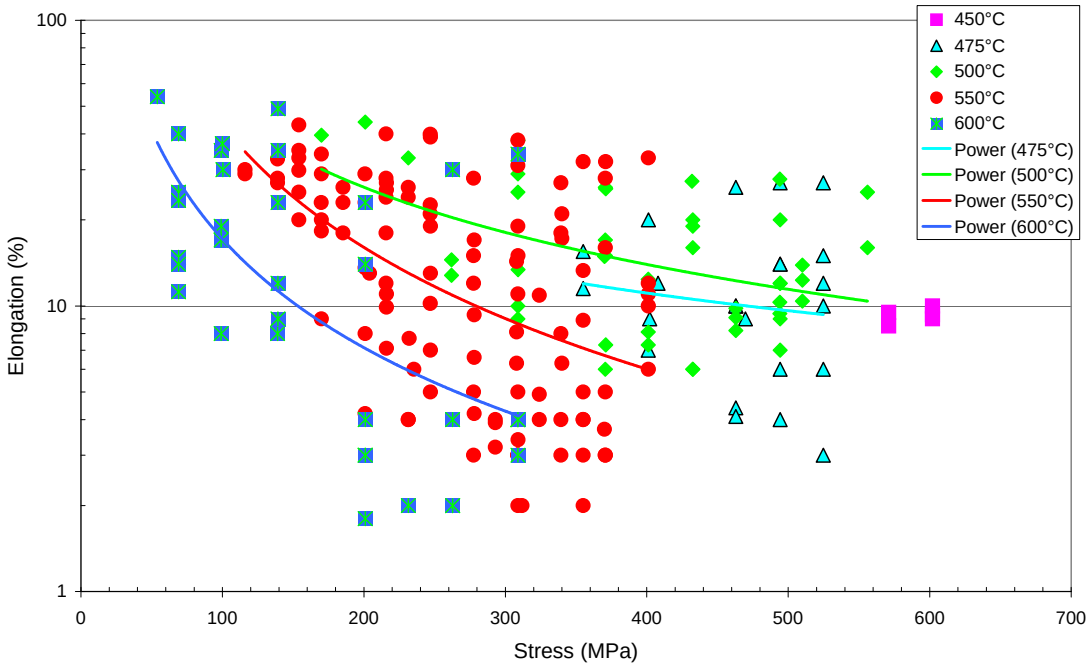

Figure 3 Elongation at Failure of 11CrMoVNbN as a Function of Stress.

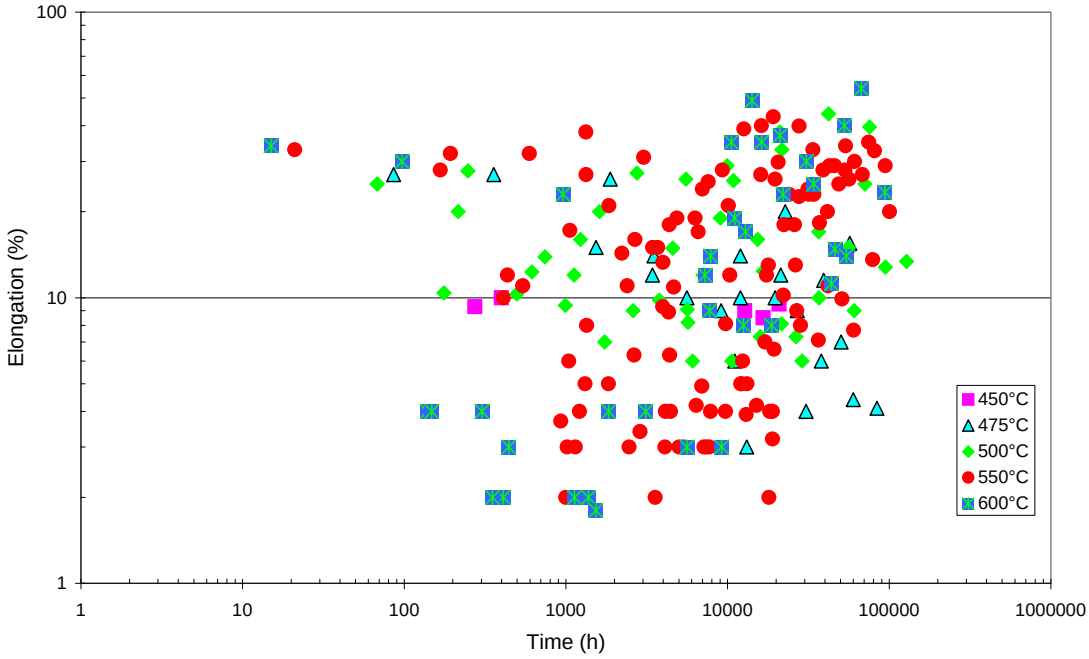

Figure 4 Elongation at Failure of 11CrMoVNbN as a Function of Rupture Time.

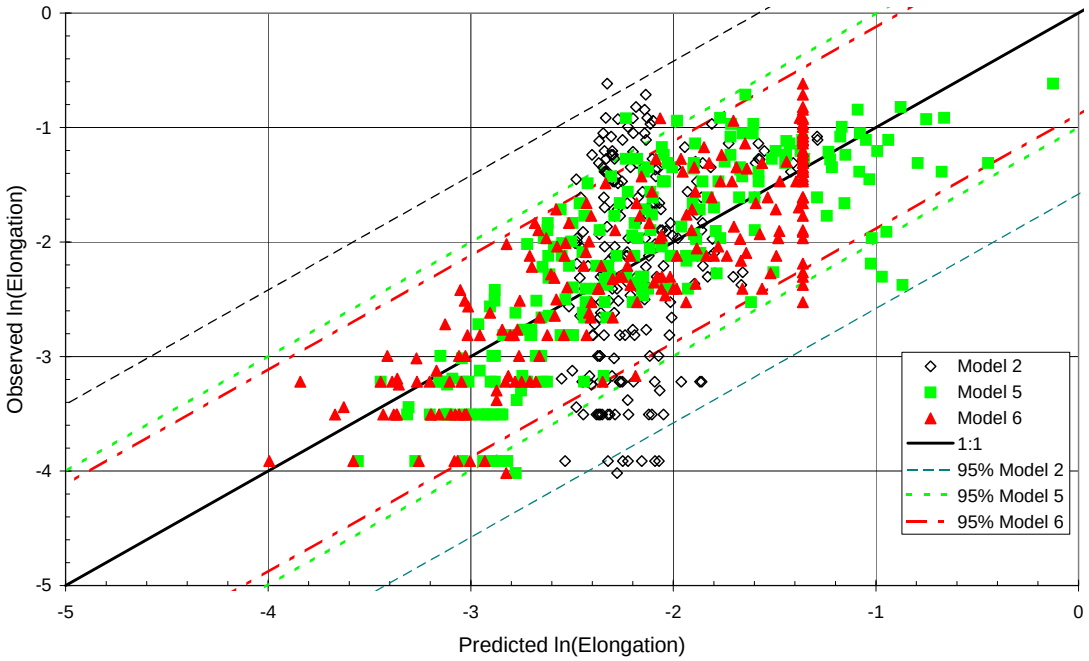

Figure 5 A Plot of Observed versus Predicted for the Elongation at Failure of 11CrMoVNbN. Showing the Values Predicted using Models 2, 5 and 6.

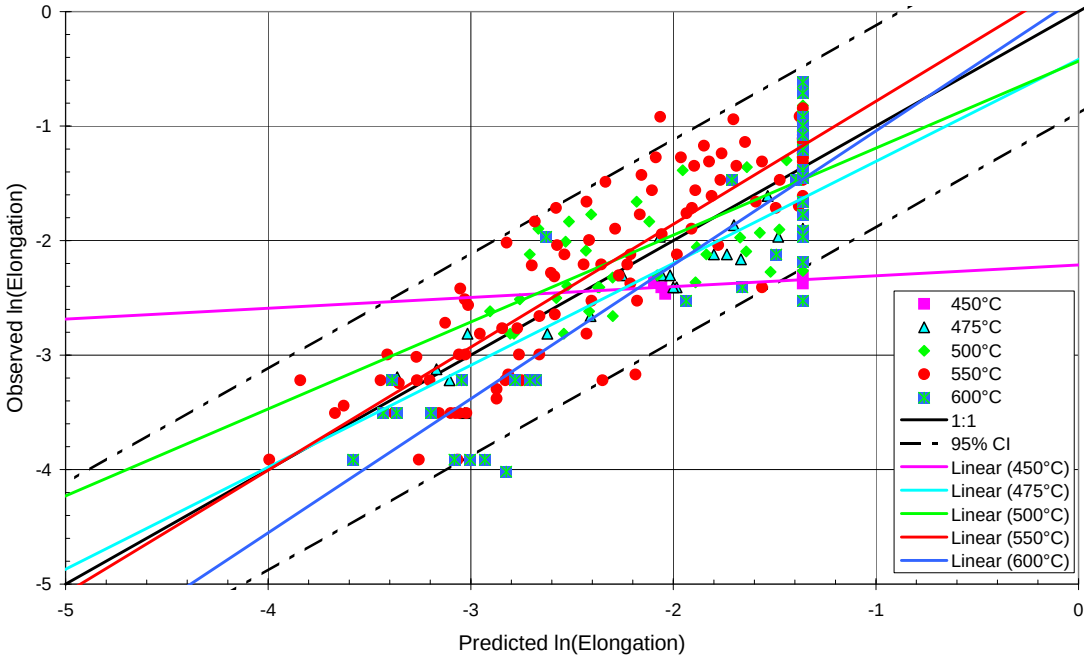

Figure 6 A Plot of Observed versus Predicted (Eq. (5), Model 6) Elongation at Failure of 11CrMoVNbN, Showing the Data at Different Temperatures.

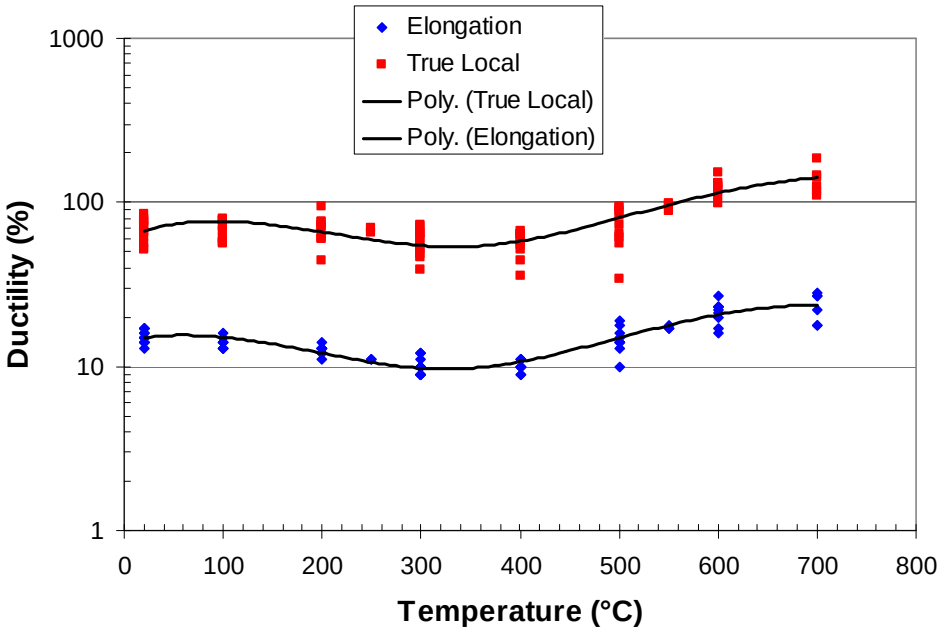

Figure 7 Ductility Measured in Tensile Tests on 11CrMoVNbN.

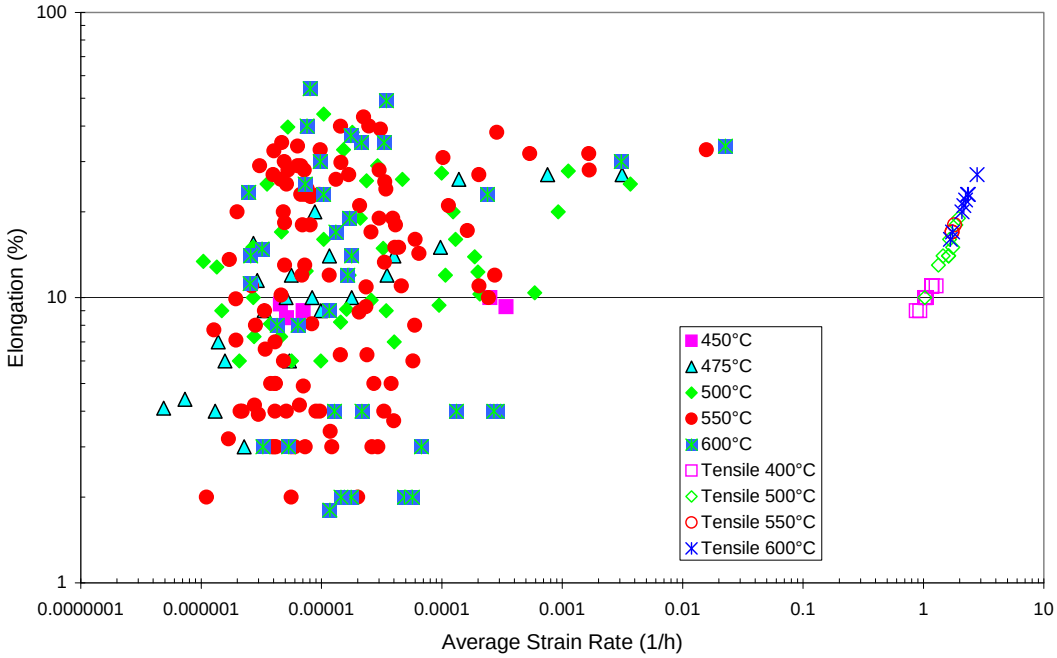

Figure 8 Elongation at Failure of 11CrMoVNbN as a Function of Average Strain Rate, Showing Both Creep and Tensile Data.

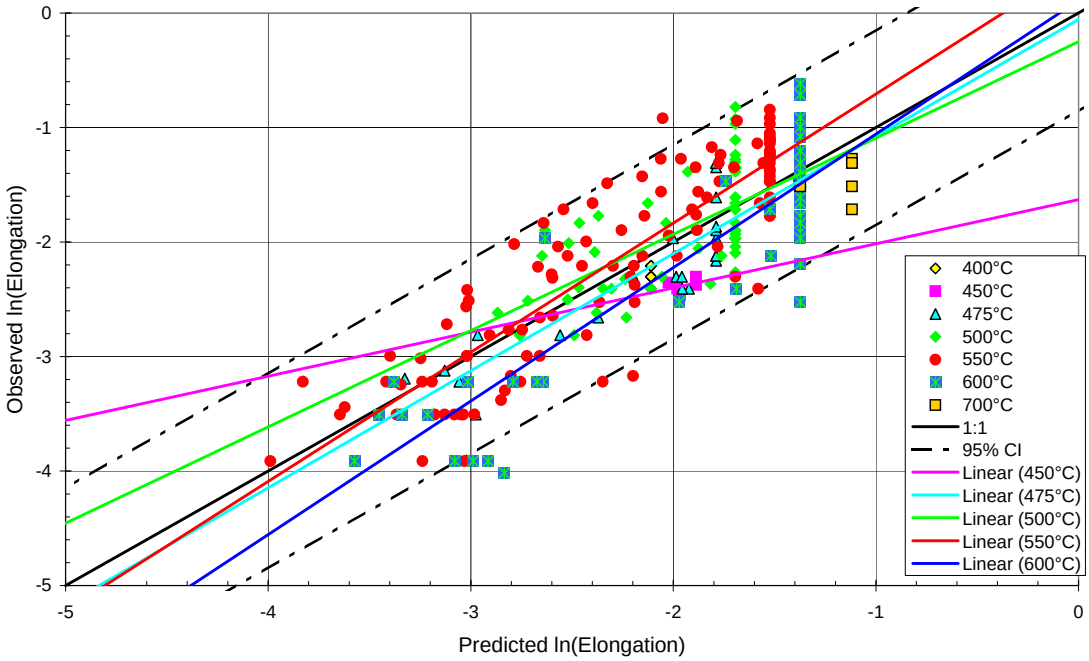

Figure 9 A Plot of Observed versus Predicted (Eq. (6), Model 7) Elongation at Failure of 11CrMoVNbN, Showing both Creep and Tensile data and Indicating Different Temperatures.

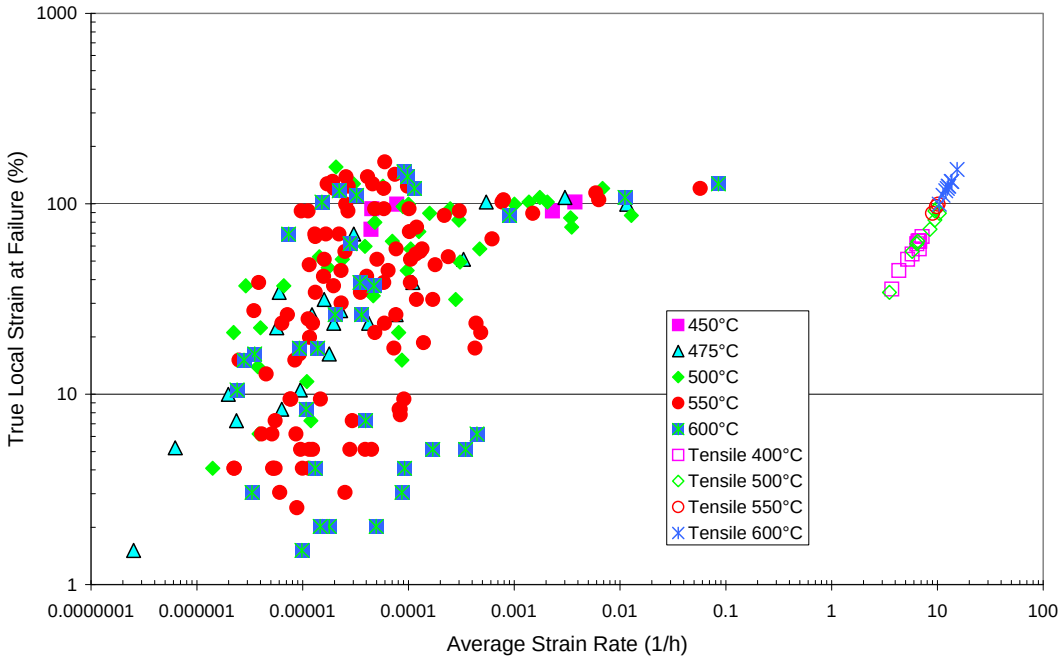

Figure 10 The True Local Strain at Failure of 11CrMoVNbN as a Function of Average Strain Rate, Showing Both Creep and Tensile Data.

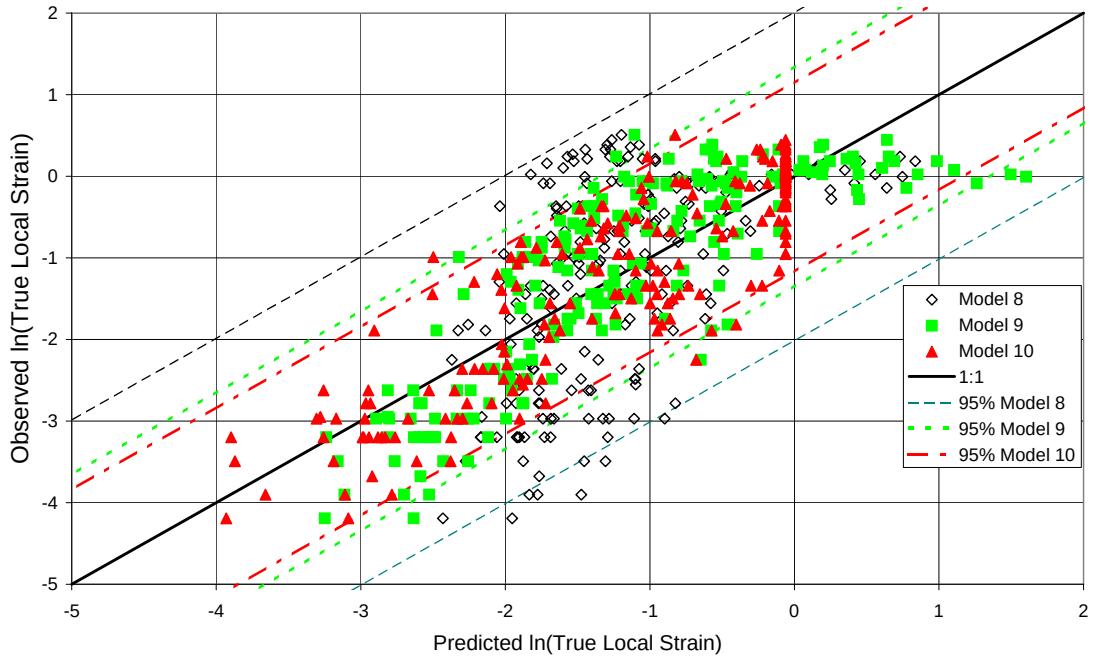

Figure 11 A Plot of Observed versus Predicted for the True Local Strain at Failure of 11CrMoVNbN. Showing the Values Predicted using Models 8, 9 and 10.

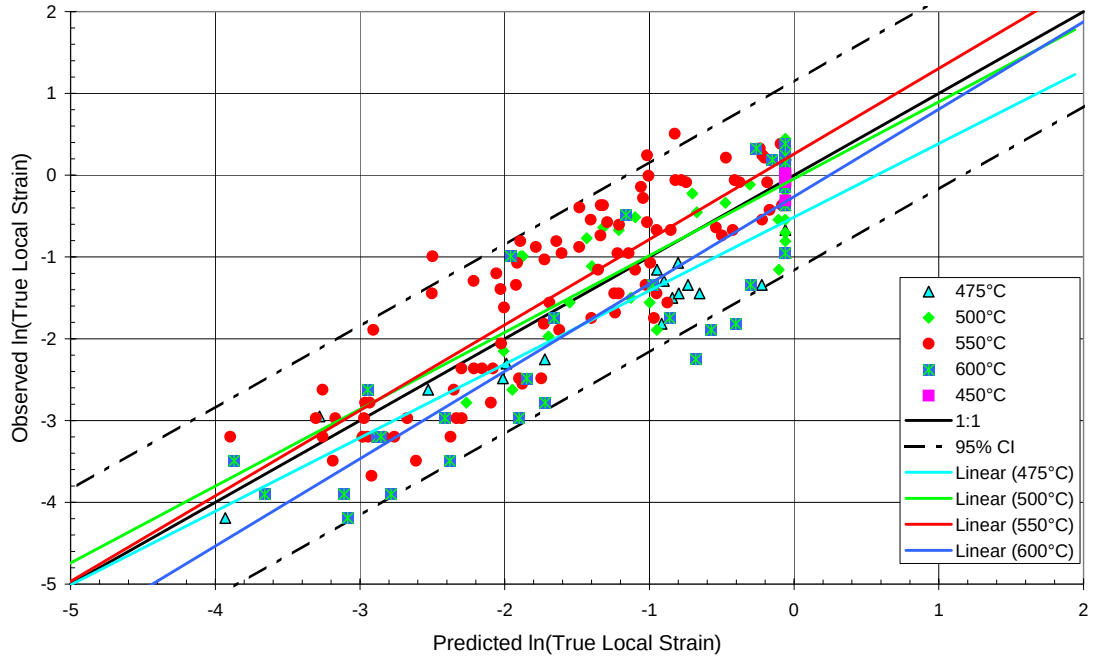

Figure 12 A Plot of Observed versus Predicted (Eq. (5), Model 10) True Local Strain at Failure of 11CrMoVNbN, Showing the Data at Different Temperatures. (Note; at 450°C all of the data are predicted to be on the upper shelf so no trend line can be fitted).

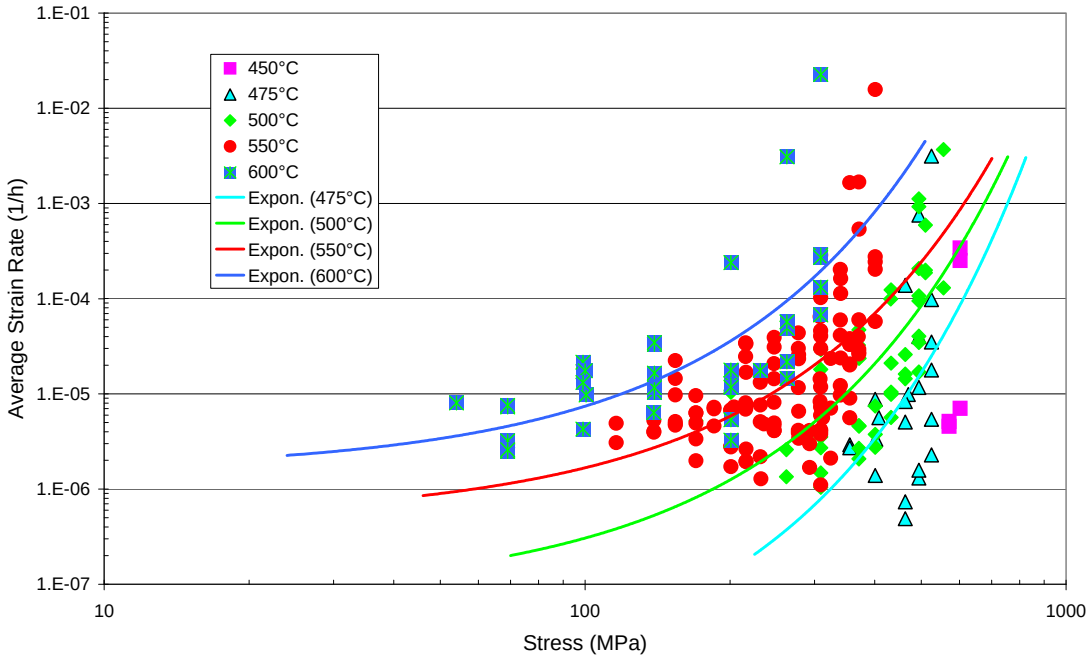

Figure 13 Average Creep Strain Rate versus Stress of 11CrMoVNbN, All Heats.

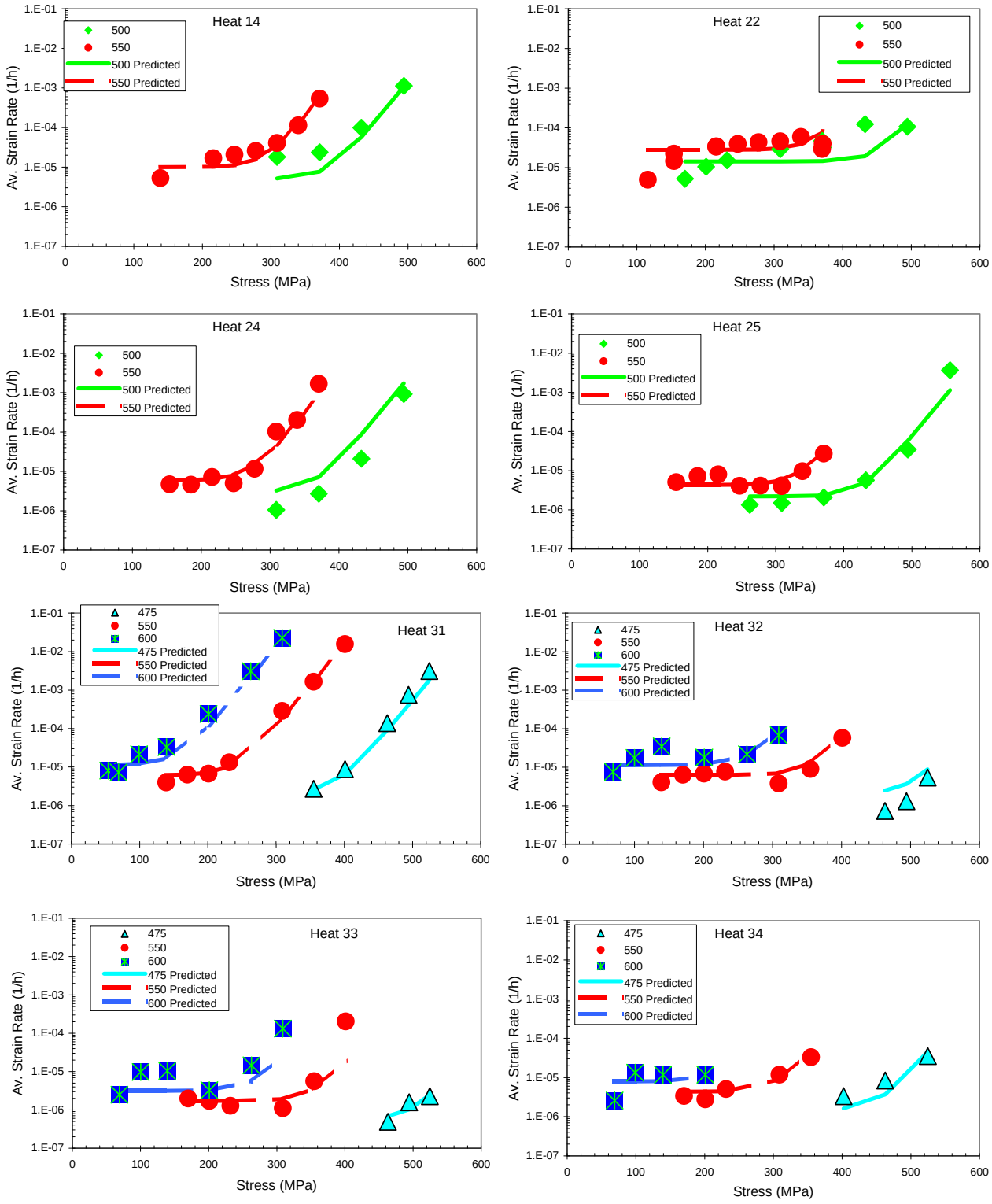

Figure 14 Average Creep Strain Rate versus Stress of 11CrMoVNbN, Specific Heats. The predictions were made using Eq. (10).

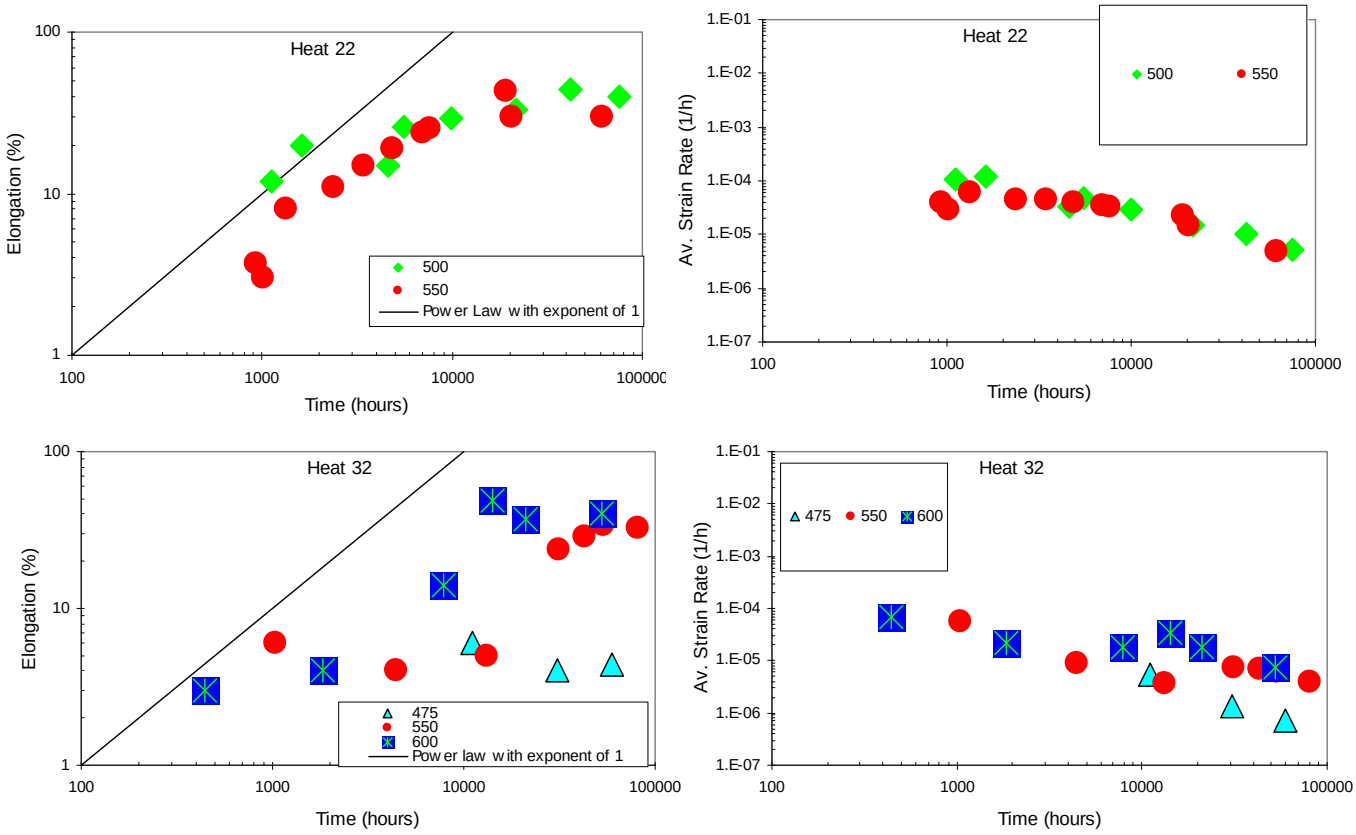

Figure 15 Ductility and Average Strain Rate of 11CrMoVNbN, Heats 22 and 32. Showing how the average strain rate does not change when the ductility increases by the same factor as the time to failure (i.e. along a power law with exponent of unity).

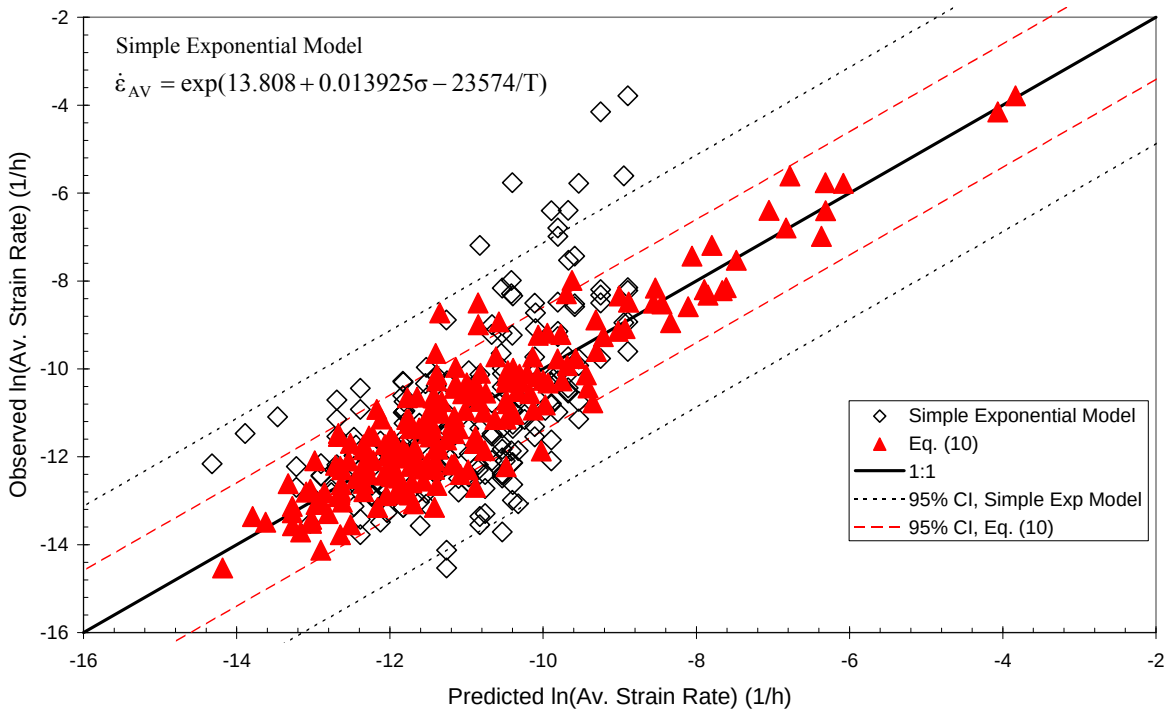

Figure 16 Observed versus Predicted Average Creep Strain Rate of 11CrMoVNbN, showing Eq. (10) and a simple exponential model.

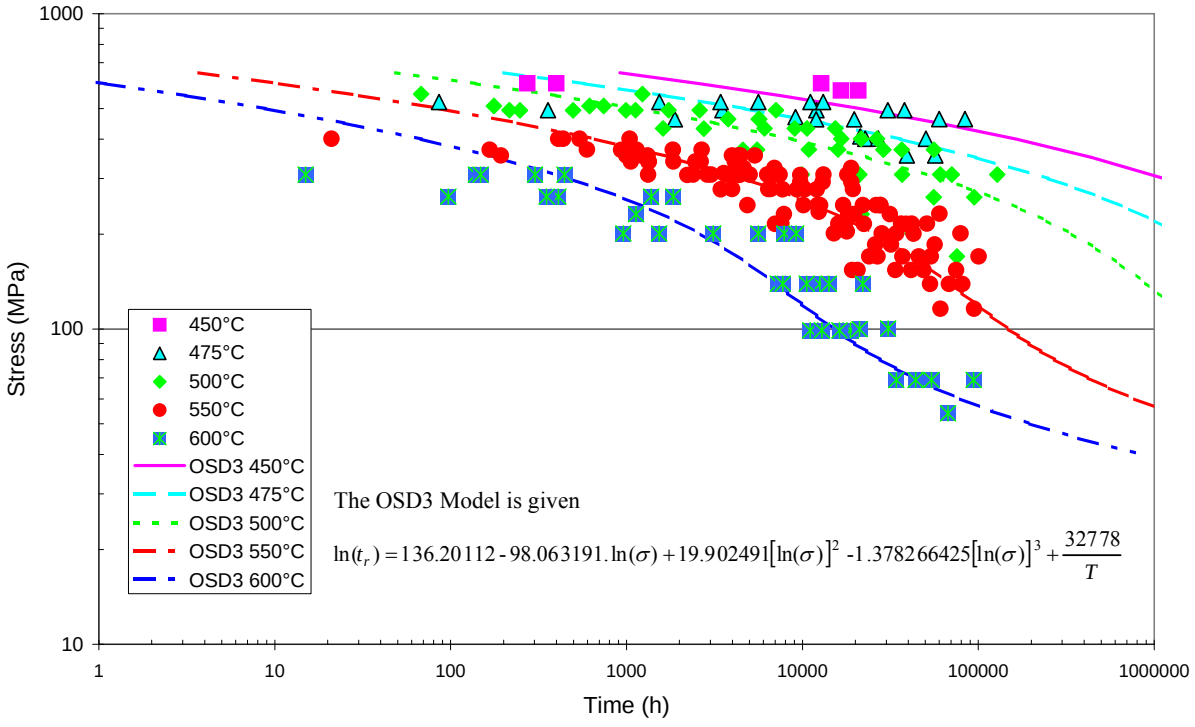

Figure 17 Creep Rupture Strength of 11CrMoVNbN fitted to a 3rd order Orr-Sherby-Dorn model

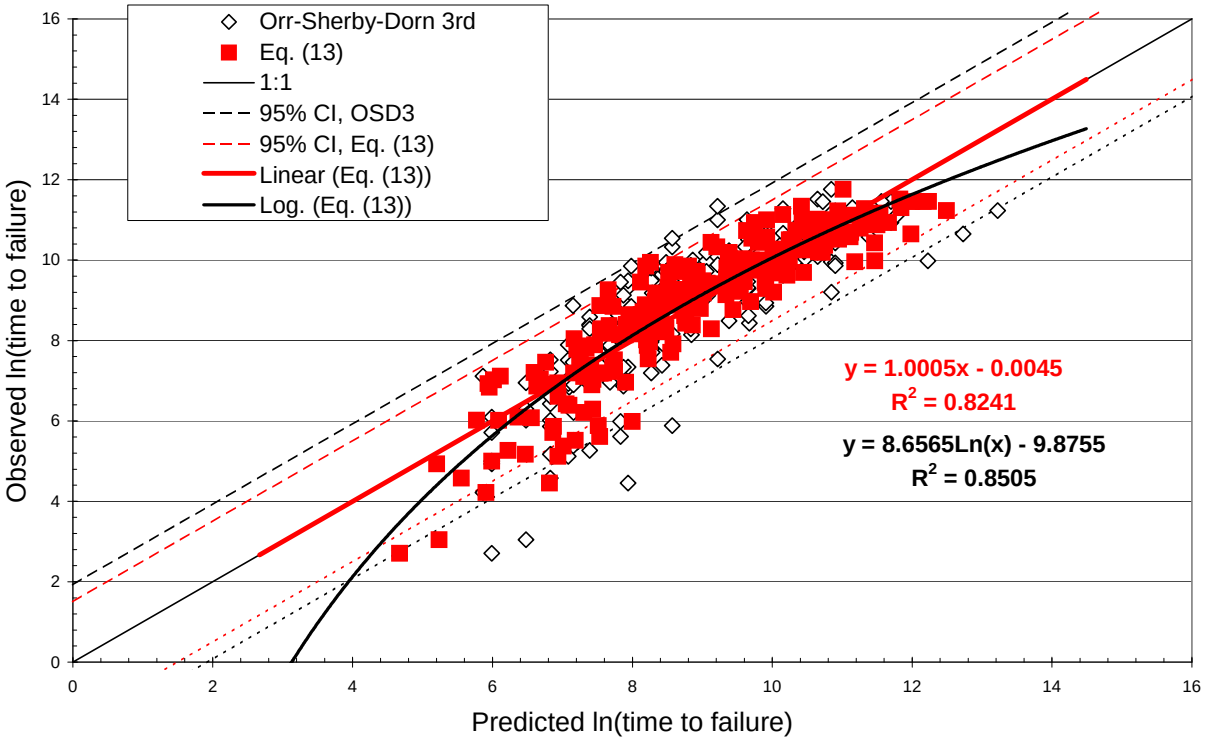

Figure 18 Observed versus Predicted Rupture Strength of 11CrMoVNbN, fitted to a 3rd order Orr-Sherby-Dorn model and to Eq. (13).

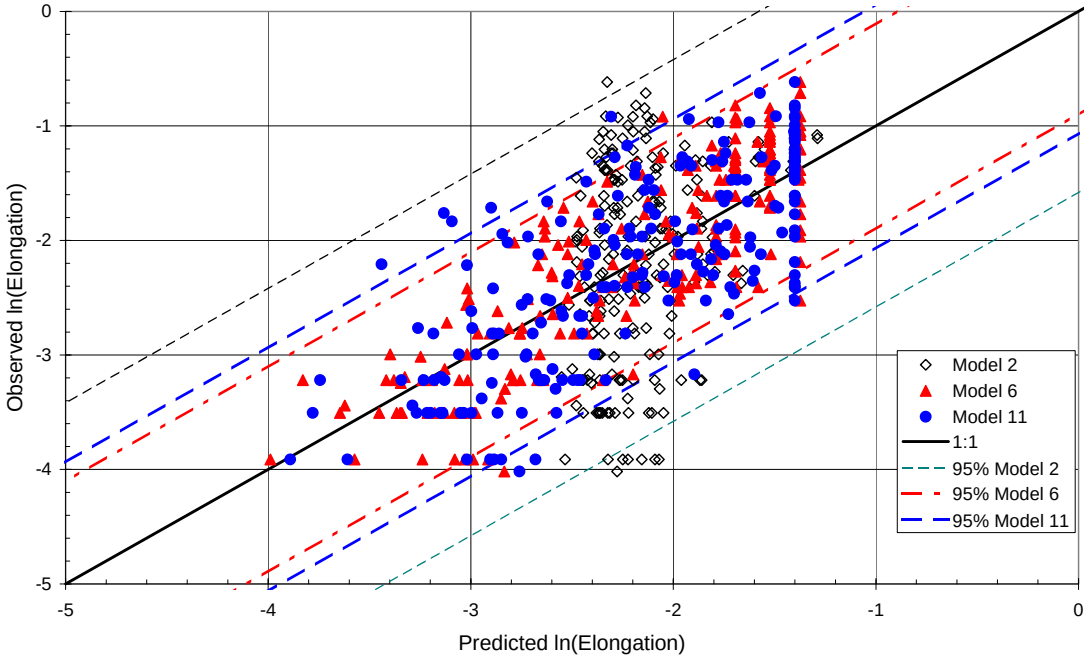

Figure 19 Observed versus Predicted Elongation at Failure of 11CrMoVNbN, The predictions were made by Eqs. (5) and (10) (Model 11). Also showing Models 2 and 6 for comparison.

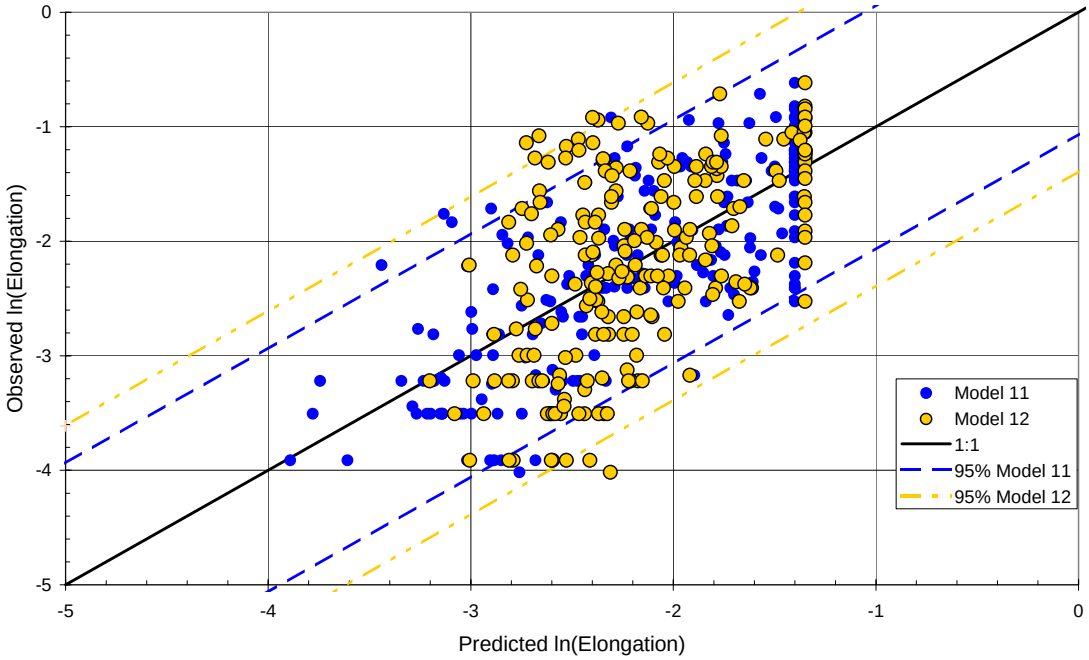

Figure 20 Observed versus Predicted Elongation at Failure of 11CrMoVNbN Using Eqs. (14) and (13) (Model 12), Also showing Model 11 for Comparison.

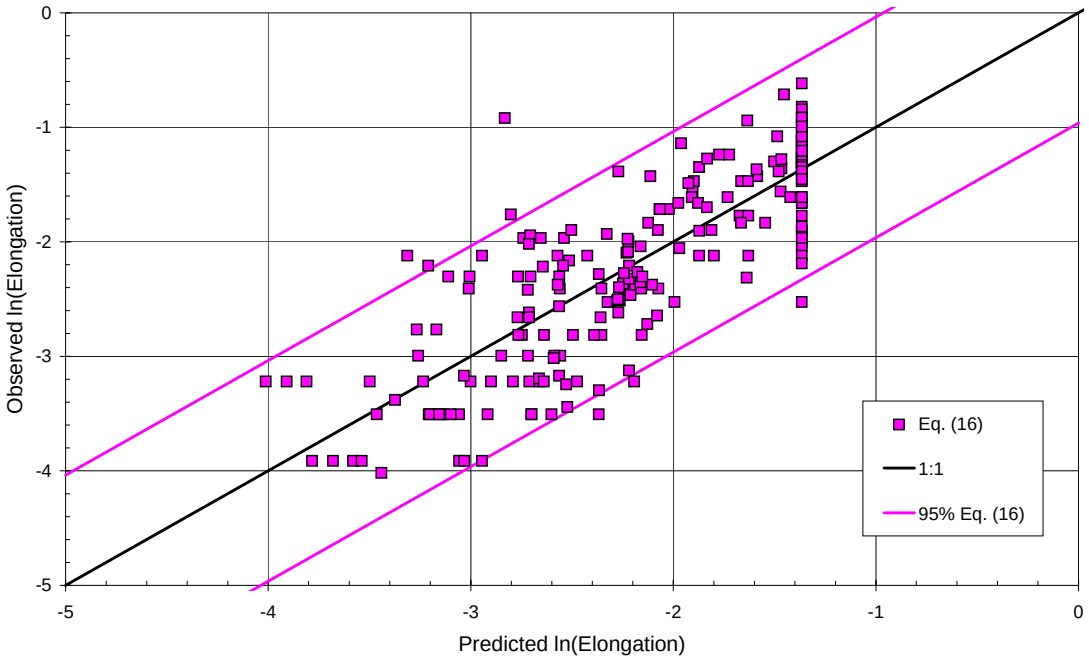

Figure 21 Observed versus Predicted Elongation at Failure of 11CrMoVNbN Using Eq. (16)

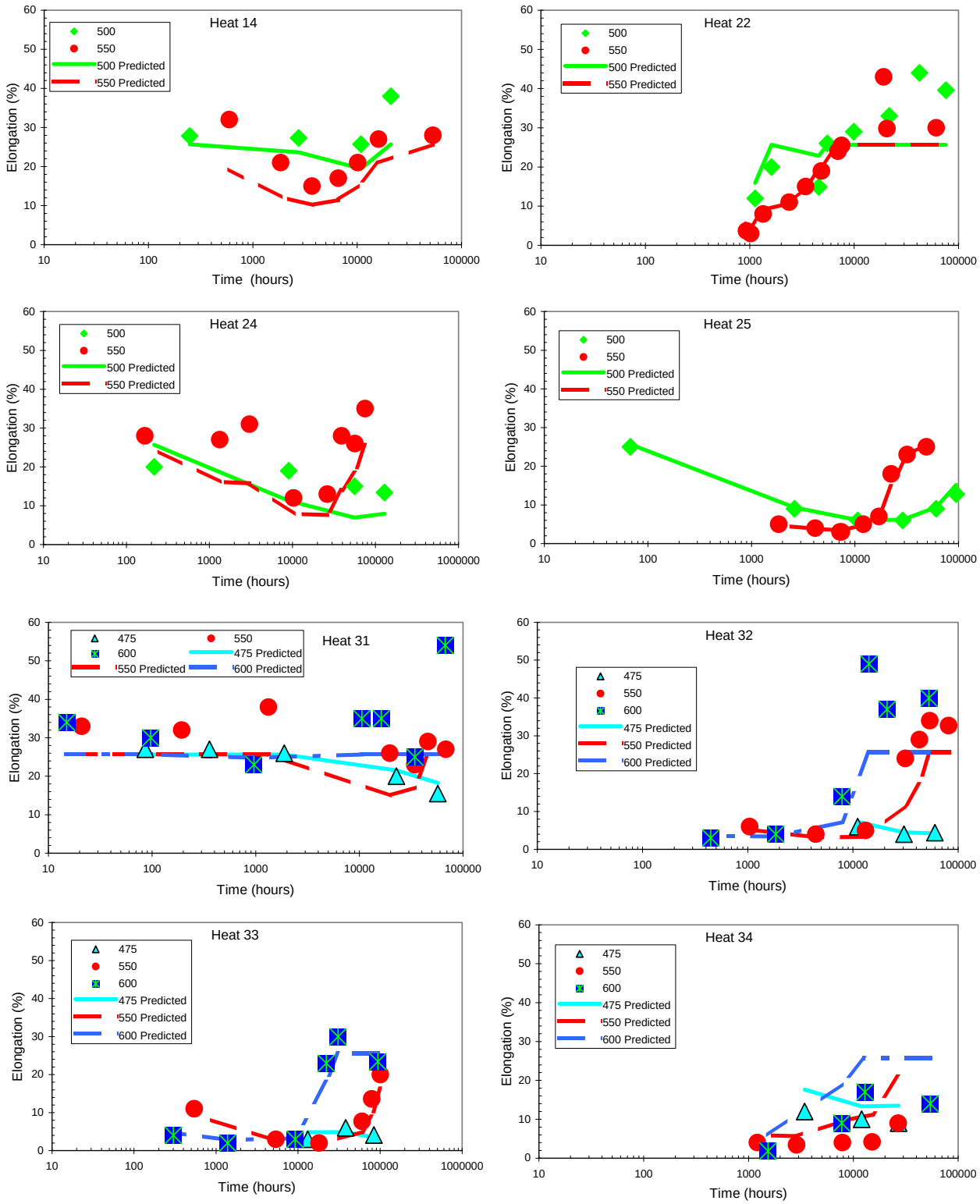

Figure 22 Effect of Time to Failure on Creep Ductility of 11CrMoVNbN for Specific Heats Eq. (5), Model 6 Fitted using the Observed Average Creep Strain Rate (note the x-axis is the observed time to failure for both the data and the prediction)**.**

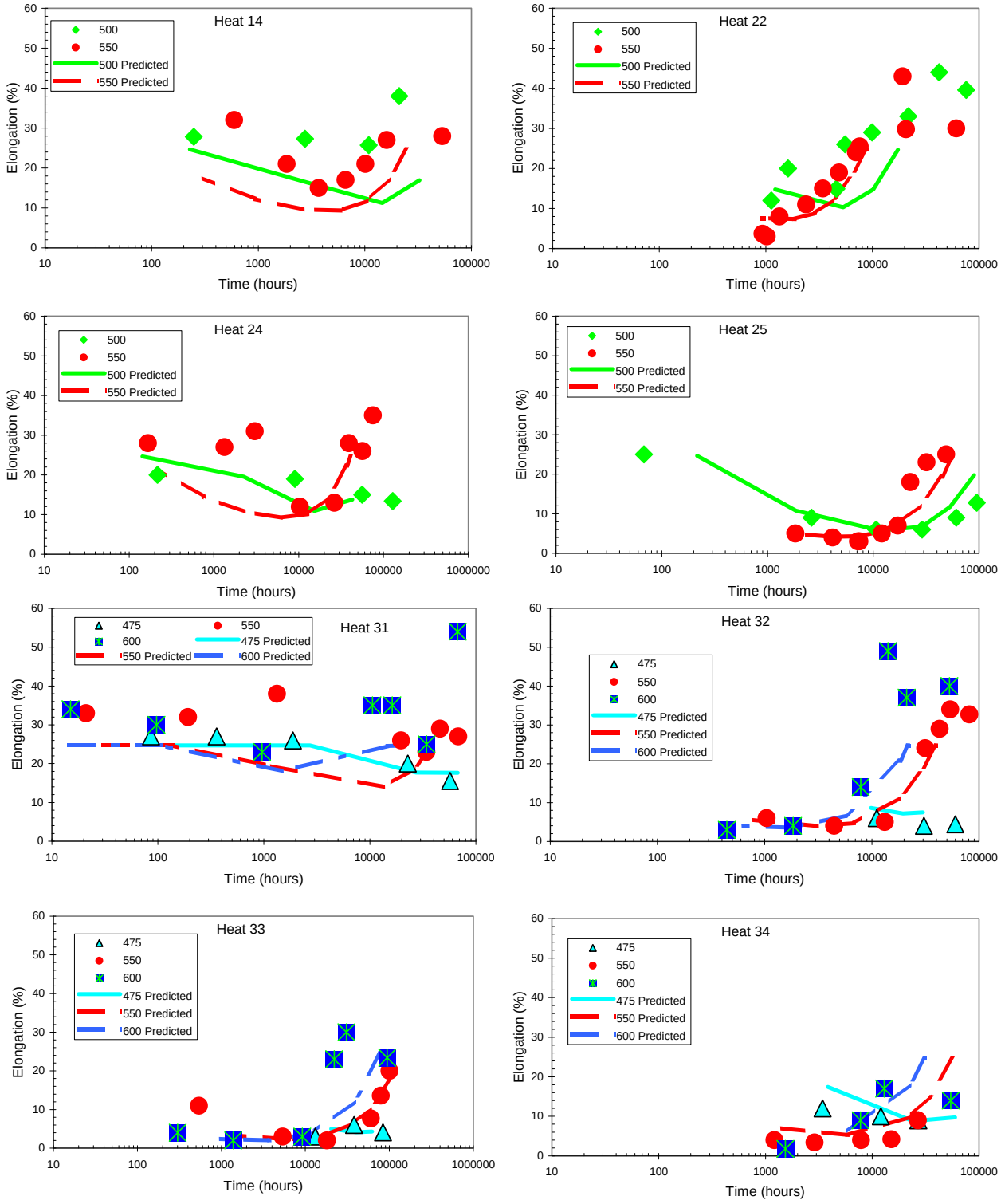

Figure 23 Effect of Time to Failure on Creep Ductility of 11CrMoVNbN for Specific Heats Eq. (5) Fitted using the Predicted Average Creep Strain Rate, Eq. (10) (Model 11). (Note; the predicted creep ductility has been plotted versus a predicted time to failure, which is Eq. (5) (Model 11) divided by Eq. (10)).

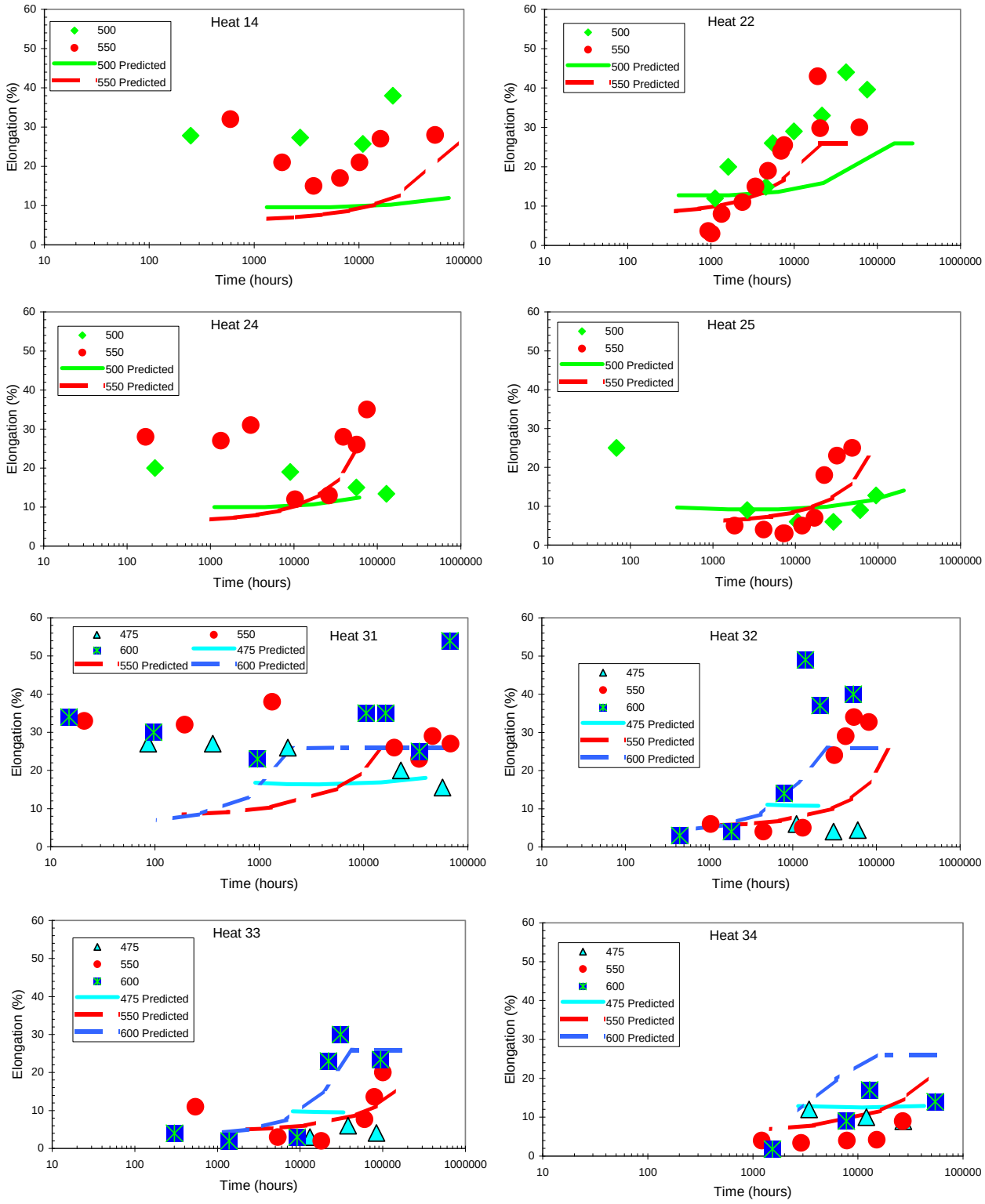

Figure 24 Effect of Time to Failure on Creep Ductility of 11CrMoVNbN for Specific Heats Eq. (14) Fitted using the Predicted Time to Failure, Eq. (13) (Model 12). (Note; the predicted creep ductility has been plotted versus a predicted time to failure, which is Eq. (13).

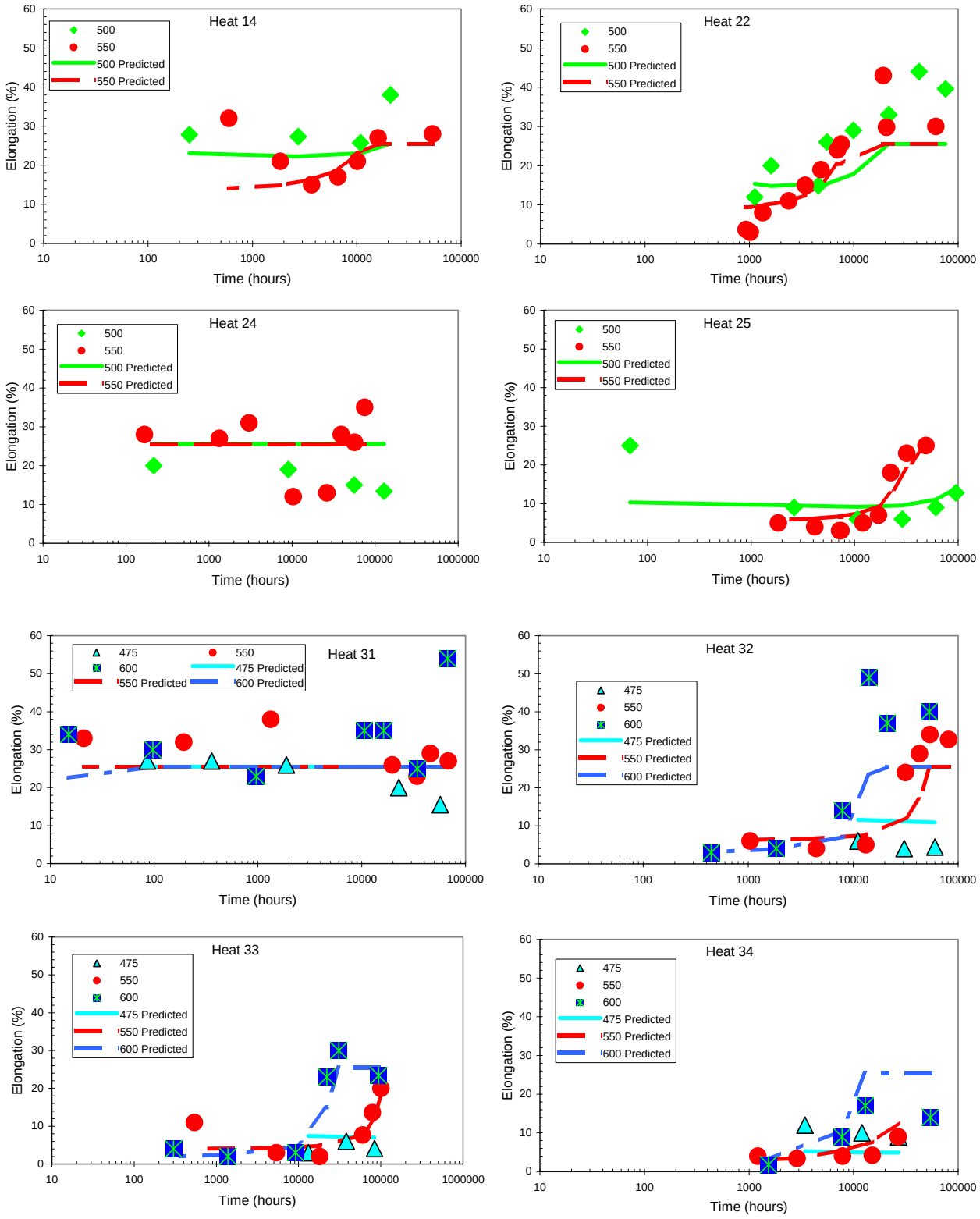

Figure 25 Effect of Time to Failure on Creep Ductility of 11CrMoVNbN for Specific Heats Eq. (16) (Model 13) (note the x-axis is the observed time to failure for both the data and the prediction).

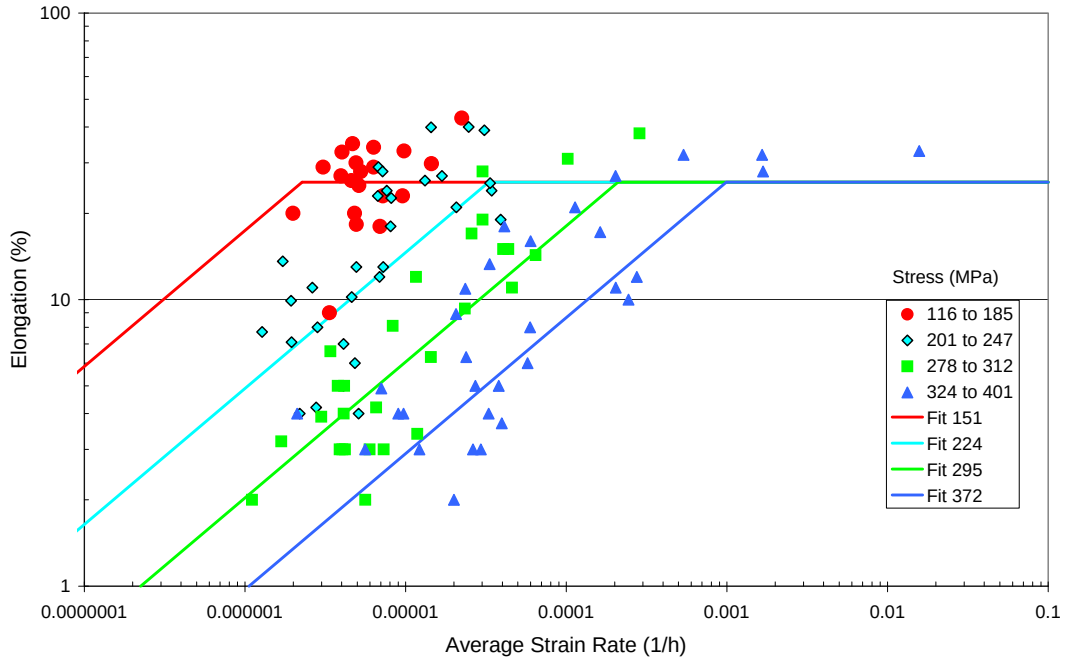

Figure 26 The 550°C Elongation at Failure data of 11CrMoVNbN, showing the Fits Given by Eq. (5) (Model 6), which have been Subdivided by Stress.

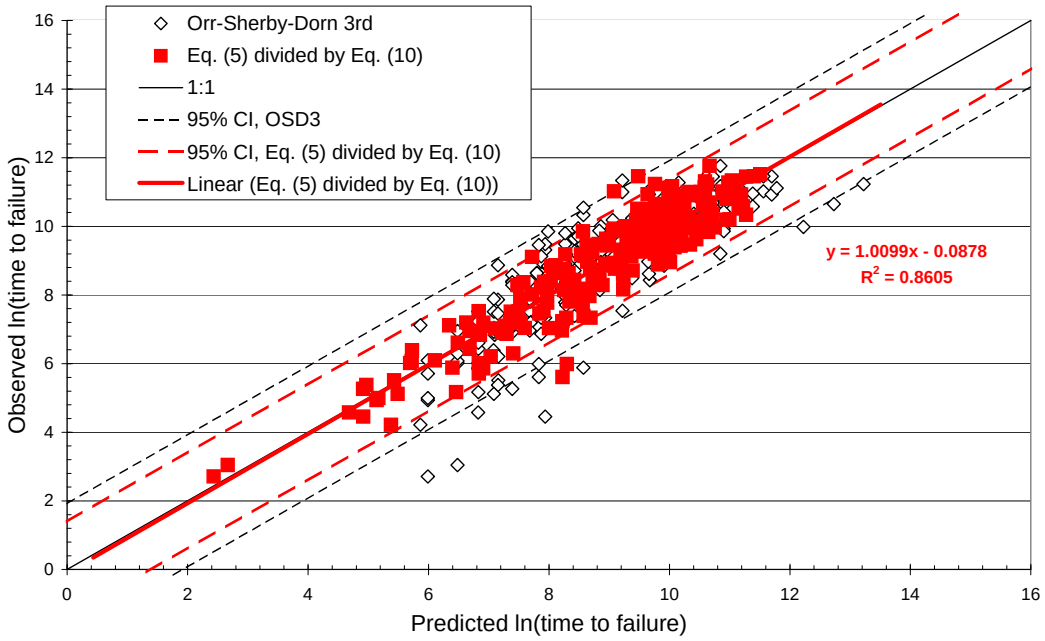

Figure 27 Observed versus Predicted Rupture Strength of 11CrMoVNbN, showing the 3rd order Orr-Sherby-Dorn model and Eq. (5) (Model 11) divided by Eq. (10).

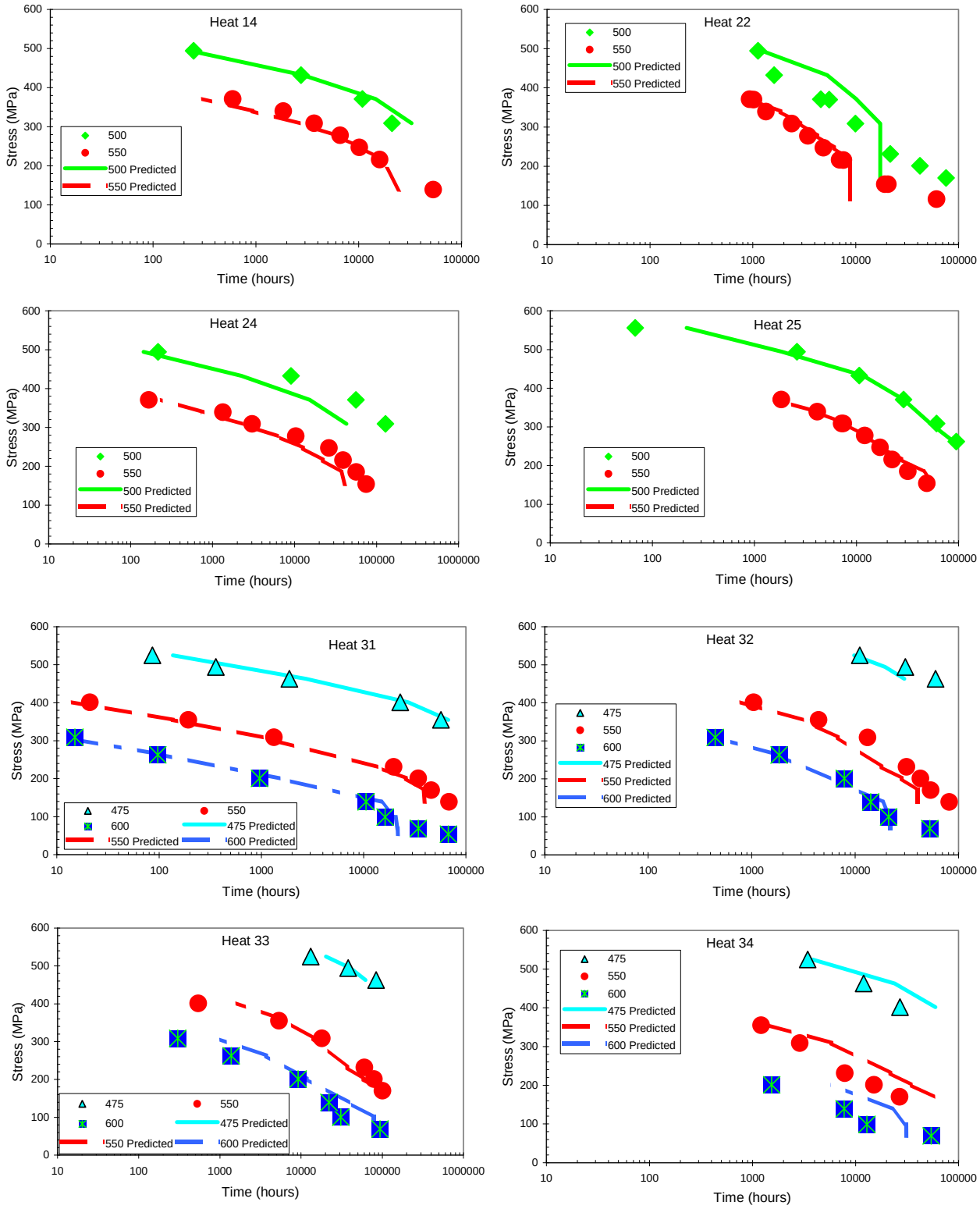

Figure 28 Rupture Strength of 11CrMoVNbN Predicted Using Eq. (5) divided by Eq. (10), for Selected Heats.

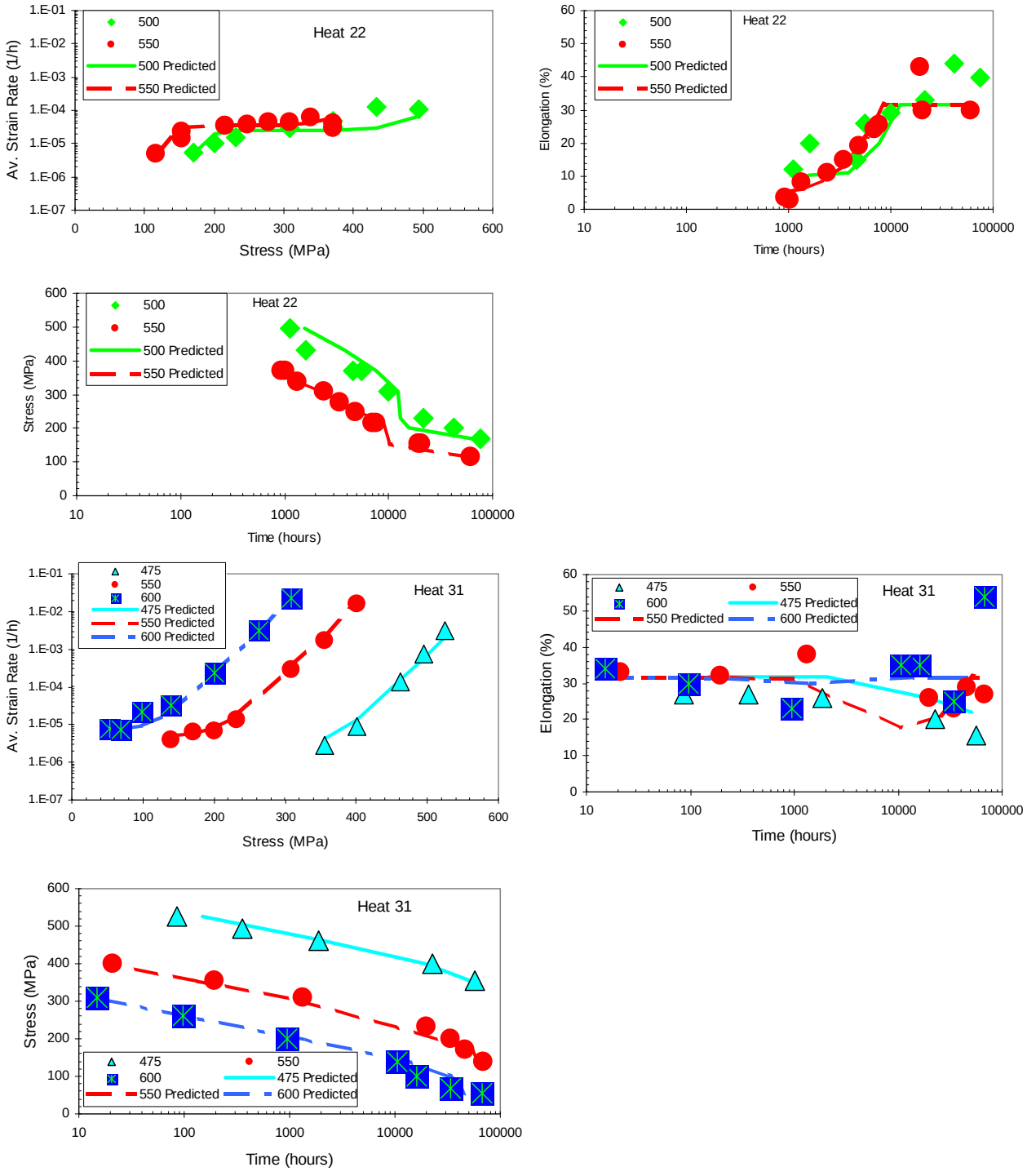

Figure 29 Results of Analyses using Metallurgical Variables to Fit the Data for two Heats Only. The average strain rates are predicted using Eq. (18) the elongations are predicted using Eq. (5) and the times to failure are predicted by dividing Eq. (5) by Eq. (18).

APPENDIX A1 DEVELOPMENT OF GUIDANCE FOR THE ASSESSMENT OF CREEP RUPTURE DUCTILITY DATA FOR ECCC

A1 INTRODUCTION

The work on the 11CrMoVNbN bolting steel, which is described in the main body of this report, used a variety of methods to analyse creep ductility. Furthermore, the author has analysed the creep ductility of many other steels. This appendix is intended to condense this experience into a procedure for performing an ECCC creep ductility assessment (CDA) that can be incorporated into a future issue of the ECCC Creep Data Validation and Assessment Procedures [A1]. The first part of this appendix describes the background to the procedure and the second part gives the text of the procedure. For consistency with the existing ECCC procedures the nomenclature that is used in this appendix conforms to that given in Volume 2 of the ECCC procedures [A1]. However, in some cases this requires new symbols, which have as far as possible been based on the system used in the ECCC procedures [A1]. It should be noted that there is scope for confusion between the nomenclature used in the main body of this report and that used in this appendix. This is particularly true in the case of the nomenclature for strain, since in the main body ε_f is used for strain at failure, whereas in the ECCC procedures this means creep strain (ε_c in the main body).

A2 BACKGROUND TO THE CREEP DUCTILITY ASSESSMENT PROCEEDURES

The aim of the statistical analysis of creep ductility data, as applied by EDF Energy, is to provide a description of the ductility as a function of the parameters that are used in ductility exhaustion approaches for the calculation of creep damage arising during strain controlled creep dwells (see Section 0).

A2.1 The Definition of Creep Ductility

In the current version of R5 [A2] the definition of creep ductility that is used to calculate creep damage using the ductility exhaustion approach is the engineering creep strain at failure, which is given by the elongation at failure, A_u, minus the initial plastic loading strain, ε_i. This definition of creep ductility is used because in austenitic stainless steels A_u often contains both ε_i and creep strain, ε_f. This is particularly true for tests on austenitic steels at relatively low temperatures such as 550 and 600°C, which are often conducted above the proof stress. The engineering creep strain at failure is used in R5 because in cases were the creep ductility is treated as a function of the strain rate then it would be non-conservative to include ε_i, which occurs at very high strain rates, with the creep strain at failure, which occurs at much lower strain rates. The engineering creep strain at failure (in absolute units) will hereafter be defined as ε_{fu} and is defined as $A_u/100 - \varepsilon_i$.

Nevertheless, for cases where a lower bound creep ductility is used that is independent of the strain rate then it does not matter that A_u often contains a component of ε_i. This is not currently an option in R5, however, it might be allowed in future issues or amendments.

In general it is found that ductility exhaustion approaches that use either ε_{fu} or A_u give conservative estimates of creep damage at failure in creep-fatigue tests. Holdsworth [A3] has suggested that a less pessimistic value of creep damage can be calculated using the local strain at failure, which is calculated from the reduction in area, Z_u. This is not currently an option in R5, however, it might be allowed in future issues or amendments. The true total local strain at failure, $\varepsilon_{tu(true)}$, can be calculated from

$$\varepsilon_{tu(true)} = \ln\left(\frac{1}{1 - Z_u/100}\right) \tag{A1}$$

and the corresponding true creep local strain at failure, $\varepsilon_{fu(true)}$, can be calculated from

$$\varepsilon_{fu(true)} = \ln\left(\frac{1}{1 - Z_u/100}\right) - \ln\left(1 + \varepsilon_i\right) \tag{A2}.$$

It is suggested that any of these four definitions of creep ductility may be used in an ECCC CDA and that the chosen one must be clearly stated, with its units (percent or absolute). For simplicity the chosen definition will be represented by the generalised symbol ε_u in much of this appendix.

A2.2 Pre-Assessment

It is anticipated that most ECCC CDAs will be performed on data sets that have been previously collated for a creep rupture data assessment CRDA. However, there are no proposals to use the information regarding the best-tested heats, which is required for a CRDA. With regards to the visual examination of the data it is proposed that, in addition to the requirements of a CRDA, plots of; (i) log ε_u versus σ_0 (or log σ_0), (ii) log ε_u versus T, (iii) log ε_u versus log t_u and (iv) log ε_u versus log ε_u/t_u. The plots will be used to identify excessive scatter and outlying data points and outlying heats. The reasons for excluding any individual data points or heats should be fully documented.

A2.3 The Assessment of Creep Ductility Data

It is usual for ECCC to demand that two independent data assessments be conducted. However, there are relatively few specialists working in this area and the proposed applications for creep ductility data are limited to specific life assessment procedures, such as R5, or for research purposes. Thus, it is suggested that a single CDA can be performed but that this should be considered as an 'informal' assessment, for the purposes of producing an ECCC data sheet. When two independent CDAs have been performed the preferred assessment can be considered as a 'formal' assessment, for the purposes of producing an ECCC data sheet.

When two assessments are conducted it is usual for the ECCC procedures to give recommendations for each of these to give similar values, otherwise additional assessments are required. There is also guidance in ECCC procedures on how to chose between the two assessments. However, the development of procedures for CDA is not advanced enough to give firm recommendations on these, at the present. Nevertheless, guidance will be given, in the procedure, regarding engineering judgements that allow CDAs to be compared and for their suitability for use in the calculation of creep damage using ductility exhaustion, to be concluded.

The assessment procedure that is given below (Section A3) is based on both the experience gained from analysing the data on 11CrMoVNbN steel and also on the experience of analysing a large number of other steels. Thus, a number of concepts that have not been discussed in this report will be included in this appendix. However, it was considered that the work on using the 'metallurgical variables' was not advanced enough to be included in this procedure. Other sources of background information on the analysis of ductility data can be found in [A1,A4,A5,A6,A7,A8,A9].

A2.4 Post Assessment Tests

In the past, assessments of creep data have all too often be conducted without questioning whether the results of that assessment are actually fit for purpose. ECCC has rectified this for CRDAs by the introduction of post assessment tests or PATs, which test the models physical realism, its goodness of fit within the range of the data and the repeatability and stability of the model in extrapolation. These tests are also valuable when choosing between assessments on the same material. The assessment procedure for CDAs that is given below (Section A3) is based on trying out a variety of different models and choosing between them. Therefore post assessment tests are integral to that procedure. However, unlike the PATs for CRDA, these PATs have not been applied to other procedures for CDA, so it is likely that improvements will be made as further work is conducted on the PATs for CDA.

The physical realism of the models (CDA PAT D1.1) can be checked visually by plotting the creep ductility versus the principal independent variable (strain rate, stress or rupture time) and by showing both the data and the predictions (see Figure 26). If temperature has been treated as an independent variable then it is necessary to clearly identify the data and predictions at each of the principal test temperatures. In addition, if strain rate and stress have both been treated as independent variables then it is necessary to use symbols and/or colour to separate the data and predictions at different conditions, as in Figure 26.

The goodness of fit within the range of the data can be assessed using plots of the logarithm of the observed ductility versus the logarithm of the predicted ductility. The first such test concerns all of the data (PAT D2.1). It should be noted that the axes for PAT D2.1, which is proposed for use with a CDA are the opposite of those used in the CRDA PAT 2.1. This change is necessary because the models used in CDA can include upper and lower shelves in which a large number of data showing random error is predicted by single values. The PAT includes fitting a line through all the observed versus predicted creep ductility data. Generally, the analysis software used to fit these lines assumes that the variable plotted on the y-axis is subject to random error and that the variable plotted on the x-axis has no error. Clearly, the observed creep ductility is subject to random error, whereas the predicted creep ductility shows no random error. Therefore, the observed creep ductility must be plotted on the y-axis and the predicted creep ductility must be plotted on the x-axis. The effect of plotting the data on the wrong axes is shown, using the data on 11CrMoVNbN, in Figures A1(a) and A1(b). The data in Figures A1(a) and A1(b) are identical, however, by plotting the data on different axes the slope of the fitted line changes from 1.00 to 0.72. It should be noted that when a least squares regression has been used to determine the creep ductility model and the dependent variable is the logarithm of the creep ductility, then the slope of the fitted line will tend to unity and the intercept will tend to zero. When other analysis techniques are used, for example maximum likelihood methods or when different error distributions are used (i.e. log-logistic or Weibull) then the slope of the fitted line will be approximately unity and the intercept will be approximately zero. Nevertheless, in some analyses of creep ductility it is necessary to make assumptions regarding the values of some of the constants and in these circumstances the slope of the fitted line may not be unity and the intercept may not be zero. Under these circumstances the best fit line on PAT D2.1 is a useful guide as to the reliability of these assumptions. It is suggested that the slope of the fitted line should be 1±0.1 and the intercept should be 0±0.3. A second use for PAT D2.1 is to assess the scatter of the chosen model. In CRDA PAT 2.1 this is done using $\pm 2.5 S_{[A\text{-}RLT]}$ boundary lines, which approximate to a 98.7% confidence interval for typical full-sized creep rupture data sets (200-500 data). The procedures for CDA may be used on both full-sized and sub-sized data sets; thus, it was decided to standardise on an actual confidence interval rather than an approximate one. This has been chosen to be the 95% confidence interval. It is suggested that the data should be reassessed if more than 5% of the data lie outside either of the 95% confidence intervals.

In addition, to testing the goodness of fit for all of the data it is proposed to test the goodness of fit at individual test temperatures (CDA PAT D2.2). For example Figure 6 includes fits to the data at individual test temperatures (rather than to all the data as in PAT D2.1. In the assessment of 11CrMoVNbN Figure 6 proved useful because it identified a problem with the data at 450°C. Thus, the proposed test would be that the fitted lines to the individual temperature should lie within the 95% confidence interval over the range of the predicted values for the whole data set. The 95% confidence interval shown in PAT D2.2 would be the same as those in PAT D2.1, i.e. they are calculated from all the data.

A2.5 References

A1 ECCC, Creep Data Validation and Assessment Procedures, Pub. By European technology Development Ltd on behalf of the ECCC Management Committee, 2005.

A2 R5, Assessment Procedure for the High Temperature Response of Structures Issue 3, EDF Energy, Gloucester, UK, June 2003.

A3 S R Holdsworth, Prediction of Creep-Fatigue Behaviour at Stress Concentrations in 1CrMoV Rotor Steel, in Life Assessment and Life Extension of Engineering Plant, Structures and Components, EMAS, UK, 1996.

A4 R Hales, A Method of Creep Damage Summation based on Accumulated Strain for the Assessment of Creep-Fatigue Endurance, Fatigue Fract. Engng. Mater. Struct.; Vol. 6, No. 2, pp. 121-135, 1983.

A5 R Hales, The Role of Cavity Growth Mechanisms in Determining Creep-Rupture under Multiaxial Stresses, Fatigue Fract. Engng. Mater. Struct., Vol. 17, No. 5, pp 579-291, 1994.

A6 M W Spindler, R Hales and R P Skelton, The Multiaxial Creep Ductility of an Ex-Service Type 316H Stainless Steel, Proc. of the 9th Int. Conf. on Creep & Fracture of Engineering Materials & Structures, ed. J D Parker, IOM London, UK, 2001.

A7 M W Spindler, The Calculation of Creep Damage as a Function of Stress and Strain Rate, Int. Conf. on High Temperature Plant Integrity and Life Extension, Robinson College, Cambridge University, UK, 14 – 16 April 2004.

A8 M W Spindler, The multiaxial and uniaxial creep ductility of Type 304 steel as a function of stress and strain rate, Mater. at High Temps. Vol. 21, pp. 47–52, 2004.

A9 M W Spindler, The prediction of creep damage in Type 347 weld metal: part 1. The determination of material properties from creep and tensile tests. Int. J. of Press. Vess. and Piping Vol. 82, pp. 175–184, 2005.

(a)

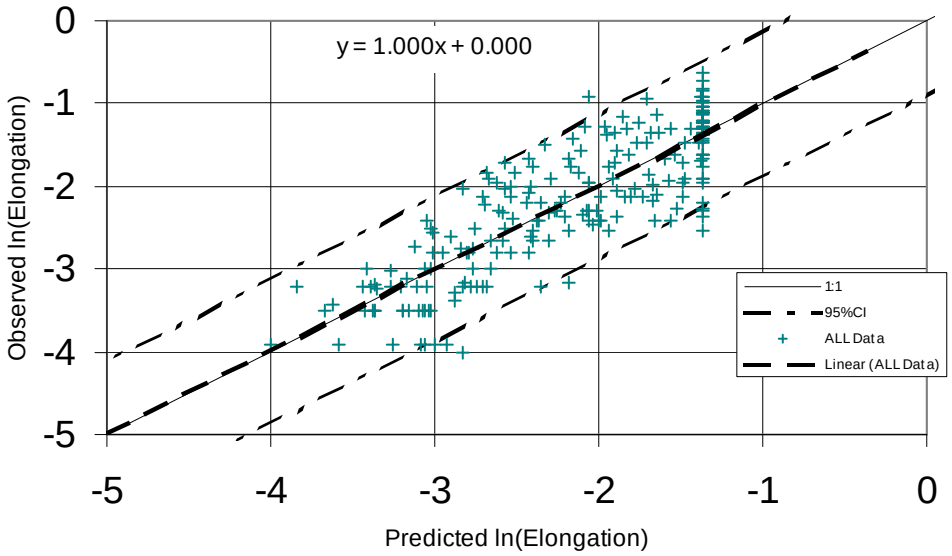

(b)

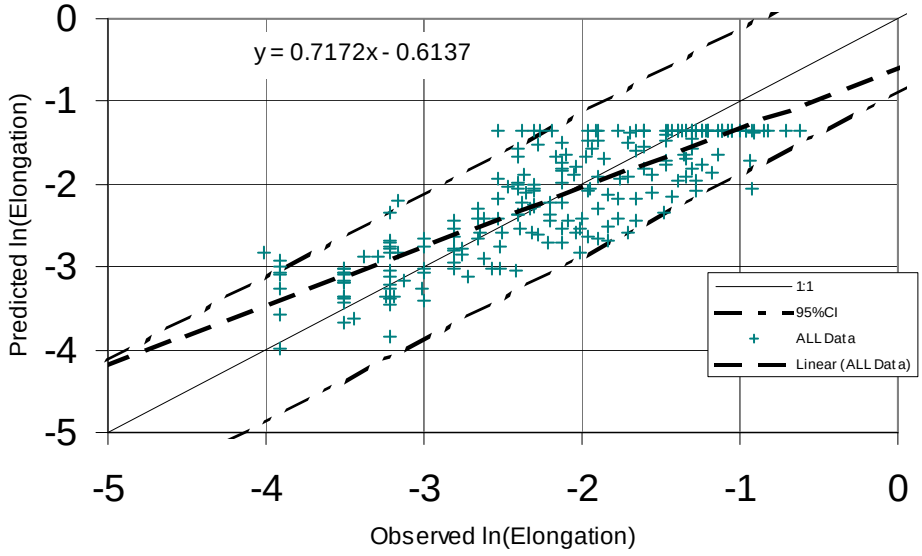

Figure A1 Graphs of Observed versus Predicted (a) and Predicted versus Observed (b) Elongation at Failure for 11CrMoVNbN Steel.

APPENDIX B

ECCC DATA SHEET FOR RUPTURE DUCTILITY

M W Spindler [EDF Energy]

blank page

APPENDIX B ECCC DATA SHEET FOR RUPTURE DUCTILITY

B1 INTRODUCTION

ECCC data sheets have been published for creep rupture and creep strain data assessments. The purpose of this appendix is to propose the format for an ECCC data sheet for rupture ductility. The proposed data sheet has been based on the format of the ECCC data sheets for creep rupture and creep strain data. However, there is currently no application for rupture ductility data in either design or material standards it is not possible to devise a data sheet that is aimed specifically at these applications. Nevertheless, rupture ductility data are used in high temperature assessment procedures and are used by steels makers, plant operators and plant manufacturers to compare and to understand the failure of materials and for design and life assessment purposes. Owing to the diverse uses that ductility data are put to the data sheet that is proposed is flexible and contains optional parts.

As an example a data sheet has been prepared for 11CrMoVNbN steel, which is based on Model 7 from the main body of this report. This example has not been endorsed by ECCC working group 3A and is purely illustrative of the proposed data sheet format, and should not be referenced as an ECCC Data Sheet.

The first page of the data sheet is mandatory as it contains details of the material's pedigree and the extent of the tensile and creep rupture data that have been included in the analysis (the tensile data are optional).

The second page of the data sheet contains numerical data that have been derived from the creep ductility assessment. The tabulated data that can be presented should be at the discretion of the ECCC working group and of the assessor. This is because different models for ductility data will suggest that different types of data are important. In this example the details of the minimum calculated creep ductility and the position of the trough in terms of stress and time to failure are given (i.e. the ductility trough). In addition, owing to the nature of the model a description of the calculation method and some cautionary notes are given.

The third page of the data sheet contains graphical data and the master equation. Once again, it is not possible to be prescriptive regarding the graphs that should be presented and whether or not a master equation is given.

The second and third pages of the data sheet can be used flexibly. For example it is only necessary to use one or other, although both can be used if required.

ECCC rupture ductility data sheet

Elongation at failure

Formal assessment: ☐

DRAFT - Steel 11CrMoVNbN

Working group: WG3X

Year: 200X

Condition of alloy to which the properties apply

	Details of materials tested				Specified ranges*	
		Units	Min	Max	Min	Max
Chemical composition	C	wt%	0.11	0.17	0.12	0.20
	Si	wt%	0.13	0.47	0.20	0.70
	Mn	wt%	0.60	1.00	0.40	1.00
	P	wt%	0.010	0.027	-	0.035
	S	wt%	0.004	0.024	-	0.015
	Cr	wt%	10.22	12.00	10.00	11.50
	Mo	wt%	0.50	0.70	0.50	0.90
	Ni	wt%	0.40	1.15	0.30	0.80
	Nb	wt%	0.24	0.48	0.20	0.55
	V	wt%	0.20	0.39	0.18	0.35
	N	wt%	0.045	0.072	0.030	0.080
Product	Form					
	Section size	mm	-	-	-	-
Heat treatment	Harden/Solution	°C	1150	1167	1100	1170
	Temper					
Tensile Properties	$R_{P,0.2}$	N/mm²	813	938	740	-
	R_M	N/mm²	964	1115	895	1050

* Specified ranges according to DIN 17240, 1976, X19CrMoNiNbVN11-1

Quantity and duration of data used in assessment

Temps	No. of	No. of	Test Durations							Minimum
°C	heats	Tensile Data Used	h <10,000	h 10,000 to 20,000	h 20,000 to 30,000	h 30,000 to 50,000	h 50,000 to 70,000	h 70,000 to 100,000	h >100,000	Elongation at failure
		Number of test points available								%
400	9	10	-	-	-	-	-	-	-	9*
450	3	-	2	2	1	-	-	-	-	8.5
475	6	-	8	5	3	3	3	1	-	3
500	9	9	23	5	5	3	3	3	1	6
550	18	3	55	21	10	12	7	4	1	2
600	6	9	19	7	2	4	3	1	-	1.8
700	6	6	-	-	-	-	-	-	-	18*
Totals	18	37	107	40	21	22	16	9	2	

( ) Figures in parentheses denote unbroken tests
* Indicates data from tensile rather than creep rupture tests

ECCC data sheet

Elongation at failure

Formal assessment: ☐

DRAFT - Steel 11CrMoVNbN

Working group: WG3X

Year: 200X

Calculated Minimum (Trough) Elongation at failure

Temps	The Calculated Minimum Rupture Ductility in %, which Occurs at Stress and Time			
	Mean	Lower 97.5% (single sided)	Stress and	Time
°C	%	%	MPa	hours
475	3.6	1.5	463	83929
500	5.7	2.4	401	26530
550	1.9	0.79	309	18042
600	2.8	1.2	263	1380

Summary details of the calculated values and cautionary notes.

The minimum elongations at failure were calculated for each of the data points, using the measured stress, temperature and average strain rate (elongation/rupture time), which are the explanatory variables.

Heats of 11CrMoVNbN steel that exhibit higher creep and rupture strength than those included in the data analysis could exhibit minimum elongation at failure values that are lower than the tabulated values.

It should be noted that the master equation would predict very much lower values than the tabulated ones for combinations of explanatory variables that involve high stress and low strain rate (longer rupture time). However, under conditions of constant load, stress or strain such combinations are not physically possible.

Signed: WG3X Convenor

ECCC data sheet

Elongation at failure

Formal assessment: ☐

DRAFT - Steel 11CrMoVNbN

Working group: WG3X

Year: 200X

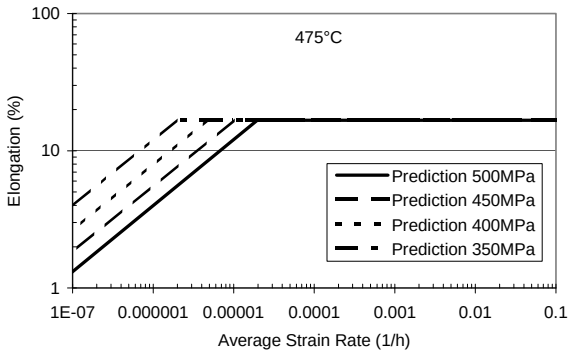

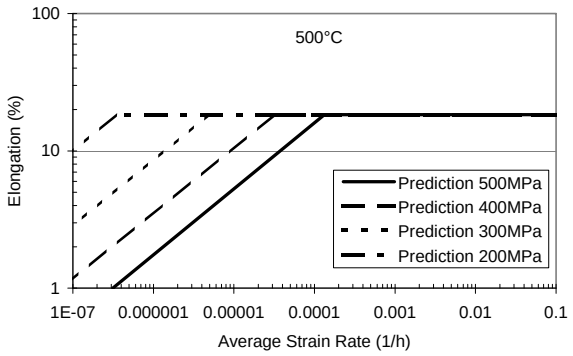

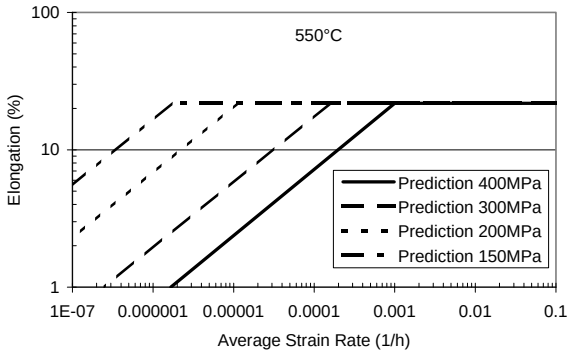

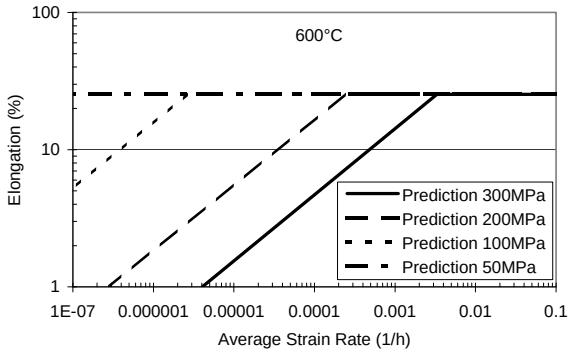

Master equation

$$\log_e(\varepsilon_u) = MIN\left[\log_e(A_1) + \frac{Q}{T} + n_1 \log_e(\dot{\varepsilon}_f) + m_1 \log_e(\sigma_0),\quad \log_e(B) + \frac{C}{T}\right]$$

where ε_u is the elongation at failure in absolute units, T is the temperature in Kelvin, $\dot{\varepsilon}_f$ is the creep strain rate in h^{-1}, σ_0 is the stress in MPa and A_1, n_1, Q, m_1, B and C are material constants. The lower 97.5% confidence limit (single sided), $\log_e(\varepsilon_{u,[L97.5\%]})$ is given by

$$\log_e(\varepsilon_{u,[L97.5\%]}) = \log_e(\varepsilon_u) - 0.8491$$

$\log_e(A_1)$	n_1	Q	m_1	$\log_e(B)$	C
-2.6205	0.4817	19114.83	-3.1378	1.1085	-2166.7